Results from the first UKMO IASI fast radiative transfer model intercomparison

Vanessa Sherlock

SISG Satellite Applications, NWP Division, UK Meteorological Office
London Road, Bracknell, Berks RG12 2SZ.

January 14, 2000

Abstract

An intercomparison of existing fast radiative transfer models (RTIASI, PFAAST) for the Infrared Atmospheric Sounding Interferometer IASI has been undertaken to select a model for use in NWP. As it is anticipated that IASI Level 1C radiances will be assimilated directly in the variational framework, both the forward model error characteristics and the accuracy of modelled Jacobians are considered.

Differences in the implementation of the fast models and differences between the line-by-line models used to generate the fast models are summarised. The impact of these differences are quantified and the implications for both future fast model developments and the specification of the forward model error covariance matrix are discussed. Fast model level 1C radiances are then compared with those simulated by each fast model's line-by-line generator for six representative atmospheres and temperature and water vapour Jacobians are compared for two extreme atmospheres (warm/humid and cold/dry) on three spectral intervals (15 μm CO_2 band, the 6.7 μm H_2O band and the atmospheric window region).

In general fast forward model error characteristics are satisfactory. On spectral intervals of interest for atmospheric sounding most channels have forward model errors which are significantly less than instrumental noise. Temperature Jacobians are also generally well described by both models. However, the models tested each have specific problems and/or limitations and revision of both models will be required before they are adequate for integration in an operational data assimilation system. Specifically, RTIASI forward model and Jacobian calculations are least accurate in the 12 to 14 μm window region and in the H_2O ν_2 band, due to the modelled water vapour absorption and the vertical resolution of the model in the upper troposphere. Further revision of the RTIASI water vapour transmittance scheme will be necessary if the magnitude, degree of correlation and state dependence of forward model and Jacobian errors compromises the information content retrievable from IASI observations. The accuracy of PFAAST Level 1C radiance calculations is compromised by the instrumental spectral response function and spectral resolution used to generate the fast model transmittance predictor scheme. The results obtained here suggest that the PFAAST fast model formulation should give satisfactory Level 1C radiance estimates if the fast model regression coefficients were regenerated using the correct IRSF definition. Given requirements for variational data assimilation, the lack of a means to generate analytic Jacobians is a serious shortcoming of the PFAAST model.

1 Introduction

The Infrared Atmospheric Sounding Interferometer IASI is to be launched on the METOP series of satellites from 2003 onwards. IASI is one of a new generation of sounding instruments with high spectral resolution ($\leq$ 1 cm^{-1}) and thousands of channels. The measurements from these high resolution instruments are expected to give significant improvements in the description of the vertical structure of atmospheric temperature and humidity fields, however accurate and efficient radiative transfer algorithms are required to exploit these observations to their full potential.

IASI is a Michelson interferometer with a maximum optical path difference (OPD) of 2.0 cm. Radiances are deduced from measured interferograms through a Fourier transform, and it is this preprocessed information which will be distributed to NWP centres and assimilated in the NWP models. In accordance with manufacturers specifications [1] the IASI instrument spectral response function (ISRF) is given by the convolution of a Gaussian with full width at half maximum (FWHM) of 0.5 cm^{-1} with a cardinal sinc function whose interferogram is a $\pm$ 2.0 cm box function: this ISRF defines the level 1C radiances.

It is anticipated that apodised channel radiances (level 1C data) will be assimilated in the Met Office NWP model either directly, via a 1D-Var retrieval or via a EUMETSAT retrieval. For the former we require:

- a forward operator H(x), in this case a fast radiative transfer algorithm, mapping model variables x to radiance observations,
- a description of the forward operator's error covariance matrix F, the observation error covariance matrix O, and the a priori background error covariance matrix B,
- the Jacobian ∇_xH(x) (or the adjoint).

These matrices are also required if channel information content is to be assessed and a subset of channels selected for assimilation.

An intercomparison of existing IASI fast models (RTIASI, developed by M. Matricardi and R. Saunders at the European Centre for Medium Range Weather Forecasting [2] and PFAAST, developed by S. Hannon, L. Larrabee-Strow H. Mosteller and W. McMillan at the University of Maryland Baltimore County) was undertaken to select a model for use in NWP. Three releases of the RTIASI code have been tested. Unless stated otherwise, the results presented here relate to the June 1999 RTIASI release. Jacobian calculations for the November 1999 release are discussed in Section 5. A single version of PFAAST, released in September 1998, has been tested.

Fast model selection was based on both the forward model error characteristics and the accuracy of modelled Jacobians. This intercomparison proved more complicated than expected: differences in the implementation of the

fast models and differences between fast model generators give variations in the calculated radiances greater than or of the same order of magnitude as IASI instrument noise. Section 3 of this report deals with the impact and implications of these differences in the fast model implementation.

Fast model level 1C radiances are then compared with those simulated by the fast model generator (line-by-line or pseudo line-by-line code used to generate the fast model transmittance predictor scheme) for six spanning atmospheres (AFGL atmospheres or an equivalent profile set). The results from these intercomparisons, which give a measure of forward model error covariance, are presented in section 4. Temperature and water vapour Jacobians have been calculated using both fast models and their generators for three spectral intervals (15 μm CO_2 band, the 6.7 μm band and the atmospheric window region) and two extreme atmospheres (warm/humid and cold/dry). These Jacobian intercomparison studies are discussed in section 5.

2 Fast radiative transfer algorithms for IASI

2.1 Basic principles of fast radiative transfer algorithms

The radiances deduced from satellite observations are given by the convolution of the incident monochromatic radiation $R(\nu)$ with the instrument spectral response function $I(\nu)$. In principle the incident radiation and intrument response can be adequately modelled and pseudo satellite observations corresponding to the NWP model state can be simulated. However, full line-by-line radiative transfer and convolution calculations are too time consuming to be used in an operational NWP data assimilation system. The fast radiative transfer algorithms used to simulate satellite observations use a polychromatic transmittance approximation: convolved layer to space transmittances τ are predicted using regression relations:

$$-\ln\left(\frac{\tau_{\mathrm{i}}}{\tau_{\mathrm{i-1}}}\frac{\tau_{\mathrm{ref,i-1}}}{\tau_{\mathrm{ref,i}}}\right) = \sum \mathrm{c_j Q_j}, \tag{1}$$

where the Q_j are the transmittance predictors and the c_j are regression coefficients determined off-line using full line-by-line transmittance calculations for a representative subset of atmospheric profiles.
These transmittances are then used to estimate the radiance R observed by the instrument:

$$\begin{aligned}\tilde{\mathrm{R}} \;=\; & \epsilon B(T_s)\tau_s + \sum_{i=1}^{N} B(T_i)(\tau_{i-1} - \tau_i) \\ & + \text{scattering and surface reflection terms.}\end{aligned} \tag{2}$$

In other words the convolution of the mononchromatic radiances is approximated by the radiance estimated using the convolved transmittances:

$$\int R(\nu)I(\nu)d\nu \simeq \tilde{\mathrm{R}}(\tau_i). \tag{3}$$

The polychromatic transmittance approximation forms the basis of all existing operational fast radiative transfer algorithms[1], but different vertical layering definitions are used for the calculation of the layer to space transmittances. Layer to space transmittances may be evaluated for layers (levels) of constant pressure (the Pressure Level Optical Depth method PLOD), or for levels of constant absorber overburden (the Optical Path TRANsmittance method OPTRAN). For fixed gases levels of constant pressure and constant absorber overburden are equivalent, but this is not the case for variable gases, in particular H_2O and O_3. The OPTRAN formulation has the advantage that, with appropriate layering, the effective layer optical depths of variable gases vary essentially linearly as a function of layer variables (pressure, temperature) and satellite viewing angle. This is in contrast to the PLOD method, where climatological variations of variable absorber amount in the layer and the overlying column give rise to marked departures from linearity, ie. the regression problem is (strongly) nonlinear. In fact, in both RTIASI and PFAAST two[2] predictor schemes are required for water vapour, with a 'switching' criteria based on the overlying water vapour column content. The performance of the OPTRAN and PLOD methods have been compared for AIRS by Hannon et al. [4]. The OPTRAN approach is not considered in detail here as it was not possible to include it in the intercomparison study in the time available.

2.2 Fast model accuracy

Naturally, the fast radiative transfer algorithm should be as accurate as possible. Ideally the errors introduced by approximations in the radiative transfer calculations:

- the prediction of convolved transmittances,
- the discretisation of radiative transfer equation (spectral and vertical resolution, and definition of the layer average temperature)
- and the polychromatic approximation

should not make significant contributions to the total observation error covariance matrix O+F. Strictly, both the channel variance and the channel error correlations must be considered[3]. In this context significant contributions are

[1] With the exception of a neural network developed for IASI and the Laboratoire de Meteorologie Dynamique[3].

[2] Note that the November 1999 RTIASI release three water vapour predictor regimes are used.

[3] The information content of the satellite observations may be reduced if forward model errors present significant channel-to-channel correlations. Although in practice it may be difficult to treat all correlations explicitly (especially where measurements on several thousand channels are to be processed), it is none the less important to characterise forward model error covariance and sources of correlated error should be eliminated wherever possible. Again, forward model error correlation should be compared with the other magor sources of correlated error: the uncertainties in spectroscopic parameters, instrumental noise correlation and undetected cloud.

those errors which are comparable to instrumental noise and spectroscopic uncertainties. Quantitative estimates of fast model transmittance errors, IASI instrumental noise and spectroscopic uncertainties are given now for reference. The impact of differences in the discretisation of the radiative transfer equation on fast model level 1C radiance simulations and forward model error characteristics will be described in detail in the section 3. Level 1C forward model errors are discussed in detail in section 4, where breakdown of the polychromatic approximation will also be mentioned briefly.

The accuracy of the fast model transmittance predictor scheme is typically characterised by comparing the convolved transmittances predicted by the fast model with convolved transmittances calculated using the generating line-by-line code (for an independent profile set). In order to quantify these differences in terms of brightness temperature fast model radiance calculations are performed twice, once using the fast model convolved transmittances and once using the convolved line-by-line transmittances. Radiances are then converted to brightness temperatures and the difference between the two spectra is calculated. These differences will be refered to here as transmittance errors. Transmittance errors for RTIASI and PFAAST, reproduced from documents diffused by the respective developers, are illustrated in Figure 1. With the exception of the ozone bands at 1050 cm^{-1} transmittance errors are generally less than or of the order of 0.1 K for both models.

CNES estimations of level 1C IASI instrumental noise (or more precisely, the diagonal elements of the O matrix) are illustrated in Figure 2. According to initial estimations illustrated with lines in Figure 2, instrumental noise will typically be less than 0.25 K in the 645 to 1500 cm^{-1} interval, and less than 0.5 K in the 1500 to 2400 cm^{-1} interval (with the exception of the 1800 to 2000 cm^{-1} interval) [5]. These noise estimates were revised by F. Cayla in August 1999 and presented at ISSWG-11 in Aix-en-Provence in September 1999. With the revised estimates, the typical instrumental noise is less than 0.3 K (but greater than 0.1 K) across the 645 to 2400 cm^{-1} interval. A marked reduction in instrumental noise (0.25 K $\rightarrow$ 0.1 K) in the 1250 to 1600 cm^{-1} interval is of particular note: in this interval forward model transmittance errors and instrumental noise are of comparable magnitude. According to Susskind and Barnet [6], IASI instrumental noise correlations are 0.71 for adjacent channels and 0.25 for channels separated by 0.5 cm^{-1}. Beyond this separation correlations are less than 0.05, and are negligible for practical purposes.

Characteristic uncertainties for CO_2 and H_2O line parameters (line strengths, line widths, temperature dependence) are discussed by L. Larrabee Strow in the AIRS Basis document [7], and a tabulated here for reference:

Gas	Line strength	Line width
CO_2	5% ΔTB $\leq$ 0.6 K	10% ΔTB $\leq$ 0.8 K
H_2O	10% ΔTB $\sim$ 0.3 K	20% ΔTB $\sim$ 0.5 K

Brightness temperature changes, as a function of wavelength, due to uncertainties in spectroscopic parameters are illustrated in the AIRS Basis document. Based on this data, uncertainties in spectroscopic line parameters will typically give brightness temperature differences of the order of 0.2 to 1.0 K, and these brightness temperature differences are expected to be correlated over 20 to 50 cm^{-1} intervals. However, it should be noted that uncertainties in modelled line shapes (far wing absorption, continuum absorption, CO_2 line mixing effects) are expected to be the dominant source of spectroscopic error. Results from studies by Amato *et al.* [8], Han *et al.* [9] and the ISSWG line-by-line intercomparison are probably more representative of spectroscopic uncertainties, particularly in the case of the 720 cm^{-1} CO_2 Q-branch and the 700 to 800 cm^{-1} interval generally (ΔTB $\sim$ 1 to 2 K), the H_2O ν_2 band (ΔTB $\leq$ 5 (10) K) and the centre of the 4.3 μm CO_2 band (ΔTB $\sim$ 2 to 10 K). A number of isolated weak water vapour lines across the IASI spectral interval also present significantly larger brightness temperature differences ΔTB $\sim$ 2 - 5 K. Nevertheless, it is hoped that ongoing experimental studies will reduce current uncertainties in spectroscopic line parameters[4] and water vapour continuum absorption, and that the development of phenomenological models will improve current descriptions of far wing absorption and line mixing for CO_2 [7].

To return then to the subject of this discussion - the definition of an upper bound to fast forward model errors - we conclude that for conservative estimates of instrumental and spectroscopic uncertainties of $\geq$ 0.2 K in both cases, fast forward model errors should ideally remain less than 0.1 K. Based on the transmittance errors reproduced in Figure 1, both fast models considered attain this level of accuracy in the vast majority of channels. However, the studies undertaken at the UKMO highlight additional sources of forward model error which were not taken into account when producing these transmittance error estimates. While the evaluation of transmittance errors is a useful means of validating a fast model transmittance predictor scheme, in the context of data assimilation it is the uncertainty in the convolved radiances simulated by the fast model(s) which must be described. In the absence of real high spectral resolution measurements convolved line-by-line radiance calculations are used to simulate IASI observations. Thus throughout this paper fast model radiance (brightness temperature) calculations will

[4] Strow suggests uncertainties in line parameters should be reduced by a factor of two [7].

be compared with convolved line-by-line radiance simulations and these IASI level 1C radiances are simulated as follows:

- a high resolution radiance spectrum is calculated using a line-by-line model,
- the interferogram of the high resolution spectrum is calculated using a fast inverse Fourier transform,
- the interferogram is apodised by the FFT of the Gaussian function and truncated at $\pm$ the nominal or modelled maximum OPD[5] depending on the simulation study,
- the apodised and truncated interferogram is Fourier transformed to give the convolved spectrum in the wavenumber (frequency) domain,
- the oversampled convolved spectrum is resampled at $\Delta\nu$=1/2L, where L is the maximum OPD, with linear interpolation where necessary,
- the brightness temperature corresponding to the convolved radiance is calculated.

2.3 Fast model efficiency

In addition to being accurate the fast radiative transfer algorithms must perform calculations rapidly enough for NWP requirements. The two fast models in question are currently installed on a UNIX workstation with multiple users, so benchmark tests are difficult to perform. Nor have the codes been optimised at compilation. For the present we simply note that there is no obvious difference in the speed of execution of either model. Subsequent speed assessments should also take input profile preprocessing steps into account.

2.4 Supplementary considerations for fast model generation and validation

The generation of fast model regression coefficients and the specification of the forward model error covariance matrix require the calculation of accurate high (spectral) resolution spectra. This is generally very time consuming if a full line-by-line model such as GENLN2 is used. Pseudo line-by-line codes (4A [10] and KCARTA [11]) have been developed which avoid many of the redundancies of full line-by-line calculations through the use of precalculated lookup tables of the absorption coefficient. The potential of these models should not be overlooked: the gain in the speed of forward radiative transfer calculations (monochromatic optical depths, transmittances and radiances) and the possibility for rapid evaluation of analytic Jacobians make these models prime candidates for fast forward model development in preparation for assimilation of IASI observations. In particular, because the detailed physics of the radiative transfer is 'hardwired' in the transmittance predictor scheme, and because the high spectral resolution observations represent an essentially new observation type one might anticipate the need to perform rapid radiative transfer calculations for tests and maybe even the rapid regeneration of the fast model. These aspects are borne in mind as we assess the impact of fast model differences: these sensitivity studies serve equally to assess the use of KCARTA as a reference model for fast model developments.

[5]Note that the maximum OPD assumed in the two fast model transmittance preditor schemes is not the same: RTIASI uses the nominal Max OPD of 2.0 cm, PFAAST uses a Max OPD of 2.074 cm.

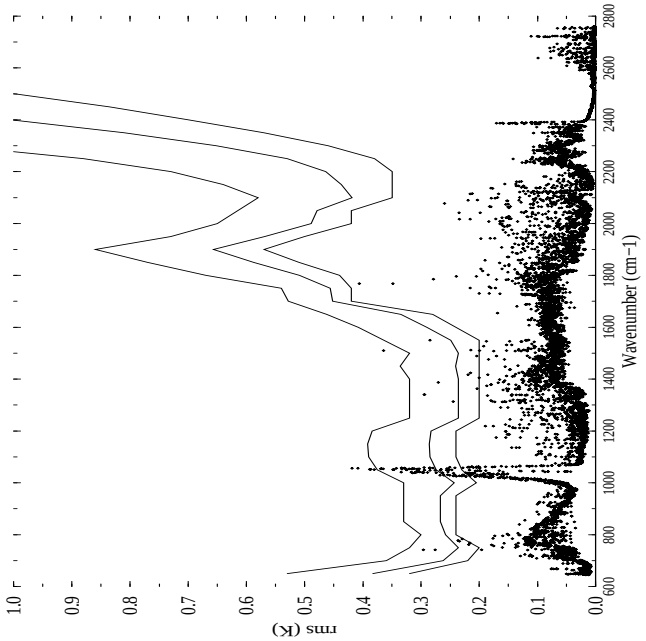

(a) RTIASI transmittance errors (independent set) and level 1C IASI instrumental noise

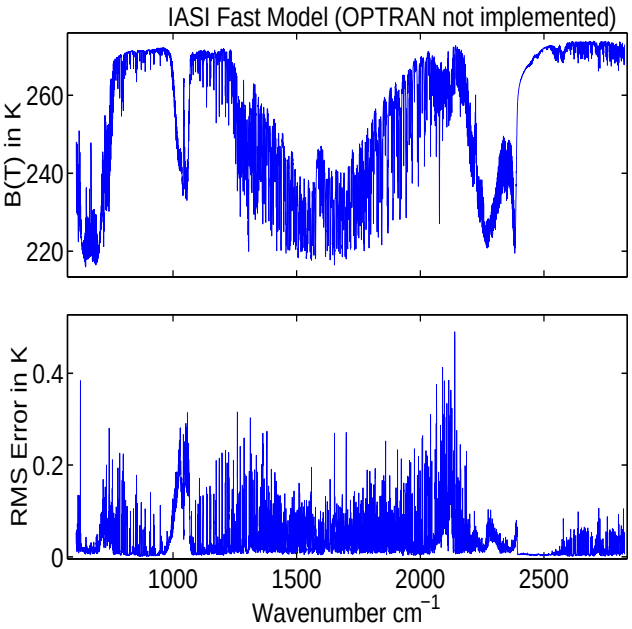

(b) A sample brightness temperature simulation and PFAAST transmittance errors (dependent set)

Figure 1: (a) Fast model transmittance errors for the RTIASI fast model (crosses) and the level 1C IASI instrumental noise equivalent brightness temperature change for the three CNES scenarios; maximum, typical and minimum noise (lines). (b) A sample fast model IASI brightness temperature simulation and transmittance errors for the PFAAST fast model (dependent set). See text for the definition and calculation of transmittance errors.

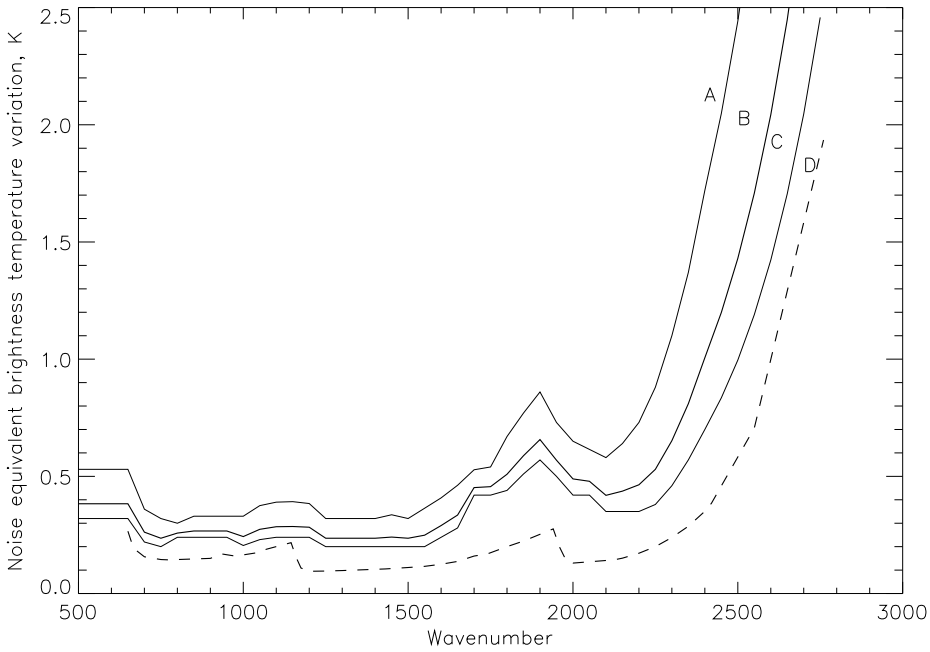

Figure 2: Level 1C IASI instrumental noise equivalent brightness temperature change for the three CNES scenarios; (A) maximum, (B) typical and (C) minimum noise (lines) and F. Cayla's August 1999 revision to the typical noise equivalent brightness temperature (dashed curve, D).

3 Impact of differences in fast model implementation

PFAAST and RTIASI both use the pressure level optical depth approach, but differ in their implementation of the method. The differences in implementation can be divided into five major categories:

- underlying spectroscopy
- absorber concentrations and vertical distribution
- modelled instrumental parameters
- discretisation of the radiative transfer equation
- regression and predictor schemes

and are summarised in Table 1. To facilitate interpretation of the results presented in the following section (and for reference for future UKMO fast model developments) the impact of differences on the modelled level 1C radiances are described briefly.

The differences in the spectroscopic data used to generate the fast model transmittance predictor schemes and the differences in the modelled absorbing atmospheric constituents (modelled gases, assumed concentration and vertical distribution) give rise to differences in convolved brightness temperatures of the order of 0.2 to 3.0 K. These differences account for many of the dominant signatures in direct PFAAST-RTIASI intercomparisons, one of which is illustrated in Figure 3. For example, the large differences in the 1200-1500 cm^{-1} and 1800-2100 cm^{-1} intervals are due to differences in the modelled water vapour continuum. Note that the CKDv2.1 continuum in the wings of the ν_2 band gives a better fit to observations [12] ie. if the CKDv2.1 continuum model is used, forward model errors between lines are generally less than 1.0 K on these spectral intervals. Significantly larger errors are observed in the P and R band heads when modelled spectra using either of the CKDv0 or CKDv2.1 continuum models are compared to observations. Thus it would be misleading to use the differences illustrated in Figure 3 to specify forward model errors for the H_2O ν_2 band.

The CFC abundances assumed in the two models differ by a factor ~ 2. Corresponding differences in modelled brightness temperatures of the order of 0.5 K are apparant at 850, 920 and 1080 cm^{-1}. The large difference in modelled CFC column abundances does not reflect uncertainites in the atmospheric CFC loadings - tropospheric mixing ratios are determined to $\pm$ 15%. The abundances assumed in RTIASI are more representative of expected atmospheric CFC concentrations at the time of launch. The situation is somewhat different when one seeks to account for the observed differences in the 15 and 4.3 μm CO_2 bands. The CO_2 column abundances assumed in the two models differ by 4%, resulting in brightness temperature differences of $\leq$ 0.4 K between 700 and 800 cm^{-1} and between 2250 and 2450 cm^{-1}. Thus while differences in the modelled CO_2 concentrations do account for some of the brightness temperature differences in the 15 and 4.3 CO_2 bands illustrated in Figure 3, there is clear evidence for additional sources of discrepancy. To the best of our knowledge these differences are not spectroscopic in origin.

The choice of spectroscopic parameters, modelled fixed gases, their abundance and assumed vertical distribution are all potential sources of differences when comparing any radiative transfer simulation with observations. Thus, while errors in the fast radiative tranfer calculations arising from these sources must ultimately be evaluated, for the present these choices will be treated as model differences and not fast model specific errors. However, given the magnitude of the resulting brightness temperature differences it is apparant that in order to characterise fast forward model errors (and identify additional sources of discrepancy) intermediary reference radiance simulations are necessary. As already mentioned, the impact studies described below concerning spectroscopy, vertical and spectral resolution and the definition of layer average temperature are also used to assess whether KCARTA can be used as a reference model to determine RTIASI forward model errors.

3.1 Quantification of fast model differences

3.1.1 Spectroscopy (line parameters)

In Figure 4 we illustrate the differences between GENLN2 and KCARTA brightness temperature simulations for the AFGL U.S. Standard Atmosphere. For the purposes of intercomparison both models were run using the CKDv2.1 water vapour continuum and GENLN2 calculations were performed with the AIRS layering definitions. A GENLN2 fine mesh grid spacing of 0.0025 cm^{-1} was used, although strictly speaking simulations were not performed on a fixed grid: for each line absorption coefficients are calculated using 10 points per halfwidth and the results are interpolated onto the fine mesh grid for the radiative transfer calculations. The small brightness temperature differences illustrated here in the centre of the 4.3 and 15 μm CO_2 band centres may be attributed to spectral resolution (this point will be addressed in more detail in following paragraphs). All other brightness temperature differences are attributed to differences in modelled spectroscopic parameters.

Model characteristics		RTIASI	PFAAST
Generating model		GENLN2	KCARTA
Spectroscopic database	line parameters	HITRAN 96	HITRAN 92, Toth H_2O line data
	H_2O continuum	CKD2.1	CKDv0
Atmospheric absorbers	modelled fixed gases	CO_2,CO,N_2O,CH_4, O_2,N_2,CFC11,CFC12	all HITRAN gases except H_2O and O_3
	gas concentrations	IPCC year 2005[a]	U.S. Std Atmosphere, CO_2 363 ppmv
RTE discretisation	vertical	43 levels	97 (101) levels
	spectral (generator)	0.001 cm^{-1}	0.0025 cm^{-1} resampled 0.00753 cm^{-1}
Apodisation	FWHM,Max OPD	0.5 cm^{-1}, 2.0 cm	0.482 cm^{-1}, 2.074 cm
Channel frequencies	$\Delta\nu$=1/2L L=Max OPD	$\Delta\nu$=0.25 cm^{-1}	$\Delta\nu$=0.241008 cm^{-1}
Predictors	number: F,W,O	10,14(14)[b],10 (levels)	7,11(2),8 (layers)
	-ve transmittances	explicit	set to zero
			weighted regression

Table 1: Summary of the principal differences between the RTIASI and PFAAST fast radiative transfer models.
a:Fixed gas profiles are taken from the AFGL U.S. Standard atmosphere, with the exception of N_2O, where an average over the six AFGL atmospheres is taken. Scaling to IPCC 2005: CO_2 ×1.1394, N_2O ×1.0094, CO ×1.0, CH_4 ×1.106, CFC11 ×1.907, CFC12 ×2.192
b: The relationship between effective optical depth and water vapour amount is often strongly nonlinear, and two predictor regimes are required. Bracketed values indicate the number of water vapour predictors used in optically thick cases (note the 'switching' criteria are not the same for the two fast models).

According to KCARTA documentation, the current KCARTA k-compressed database of absorption coefficients is based on HITRAN92, with CO_2 line mixing from GENLN2. In this case, with the exception of the CO fundamental at 2145 cm^{-1}, brightness temperature differences due to differences in modelled spectroscopic parameters should less than 0.1 K throughout the spectral interval illustrated. However, it has become apparant through email communication with the group at UMBC that line parameters for water vapour lines from Toth were appended to the HITRAN92 database when generating the KCARTA k-compressed database (S. Hannon, private communication). Note that these water vapour line parameters are not included in HITRAN96, and no literature reference for the lines has been supplied.

In all cases, brightness temperature differences in excess of ± 0.5 K are associated with water vapour lines. Figure 5 and the accompanying table illustrate the effects of the modelled line widths on layer-to-space water vapour transmittances in the 795 - 800 cm^{-1} interval. Toth air broadening coefficients differ by factors of 1.1 to 2.5 compared to their HITRAN96 equivalents and the effects of self broadening are modelled. The corresponding differences in brightness temperature range from 0.1 to 3.0 K. Both the line width differences and the resulting brightness temperature changes are significantly larger than the characteristic spectroscopic uncertainties quoted earlier.

Radiances calculated using the two sets of spectroscopic parameters could usefully be compared with observations to determine which gives a better description of the observed absorption. In the mean time, these large differences in line parameters do limit the use of KCARTA for the validation of RTIASI.

3.1.2 Spectral resolution (generator)

In Figures 6(a) and (b) the impact of differences in the spectral resolution used to simulate the high resolution spectra are illustrated. In Figure 6(a) the impact of differences between the RTIASI generator resolution and the nominal KCARTA resolution are investigated. GENLN2 was run with a fine mesh grid of 0.001 cm^{-1} and 0.0025 cm^{-1} resolution, although the latter is not strictly equivalent to the KCARTA spectral resolution because the KCARTA k-compressed absorption coefficients are generated at 0.0005 cm^{-1} resolution and averaged to 0.0025 cm^{-1} resolution. Brightness temperature differences in the 645 to 800 cm^{-1} interval are of the same magnitude as forward model transmittance errors. Smaller brightness temperature differences are observed in the 4.3 μm CO_2 band centre and in the O_3 ν_3 band.

When generating the PFAAST transmittance predictor scheme KCARTA layer to space transmittance spectra were resampled (with linear interpolation) at $\Delta\nu$=0.007533 cm^{-1} **before** the inverse FFT and apodisation. The effects of an equivalent resampling of radiance spectra before apodisation are illustrated in Figure 6(b). Changes of up to 0.5 K in level 1C brightness temperatures are observed in the spectral intervals described above when compared to those calculated from spectra at the original 0.0025 cm^{-1} KCARTA resolution. Differences also occur in the H_2O ν_2 band, but generally remain $\leq \pm$ 0.05 K. These errors give rise to a bias on a channel-by-channel basis when the brightness temperature differences for a number of atmospheric states are analysed (ie. they are not random) and are spectrally correlated: for example, the largest differences occur in the 15 μm band and are

associated with the description of local maxima and minima of variations in the brightness temperature of an amplitude of $\sim$ 10K and with characteristic spectral scales of the order of 0.5 cm^{-1}.

3.1.3 Vertical layering

In Figure 7 the effect of the choice of layering (vertical discretisation) is examined. GENLN2 radiance calculations were performed with the layering definitions used to generate the RTIASI transmittances and compared with the identical simulation, but with the AIRS/PFAAST layering definitions. The difference in level 1C brightness temperatures are illustrated for the AFGL U.S. Standard atmosphere. Differences in layering have a clear impact across the H_2O ν_2 band (with maximum differences in line centres) and in the 4.3 μm band centre. Smaller variations in brightness temperature are observed in the 15 μm band. The magnitude of the brightness temperature differences does depend on atmospheric state and in particular, on the vertical gradients of water vapour and temperature in the upper troposphere and lower stratosphere. Differences are greater in the 15 μm band ($\leq$ 0.1K) and the 6.7 μm band ($\leq$ 0.3K) for the AFGL tropical atmosphere because this atmosphere has a well defined tropopause (in contrast to the U.S. Standard atmosphere for example, which has an extended isothermal layer in the (lower) stratosphere). In both cases the sign of the differences is the same: the simulated brightness temperatures are warmer for the 43 level atmosphere.

3.1.4 Definition of layer average temperature

In the discretised radiative transfer equation (Equation 3) the contribution from a given atmospheric layer to the observed radiance (in a given channel) is given by $B(T_i)\Delta\tau$, where B is the Planck function and T_i is some characteristic temperature for the layer i. Three definitions of T_i are encountered:

- a simple arithmetic mean of the bounding level temperatures, as in RTTOV,
- an air density weighted mean temperature, as in RTIASI, PFAAST and KCARTA,
- a Curtis Godson absorber weighted mean temperature, as in GENLN2.

Absorber density and temperature will generally both vary across a layer. The layer average temperature T_i should therefore characterise the mean temperature of the absorbing molecules: this is the basis of the Curtis Godson approximation. For uniformly mixed gases the second and third definitions of the layer average temperature are strictly equivalent, however for gases like ozone and water vapour this is not the case.

Figure 8(a) illustrates the difference between RTIASI layer average temperatures and the Curtis Godson absorbed weighted layer average temperatures for CO_2, H_2O and O_3, as calculated by the GENLN2 layering subroutine for the AFGL Tropical (1) and U.S. Standard (6) atmospheres. As expected of a uniformly mixed gas, the RTIASI and CO_2 weighted layer average temperatures (dotted line) are identical. Significant differences in the layer average temperature are observed between air density and H_2O and O_3 weighted layer average temperatures;

- where the vertical variation of absorber density differs from that of the total air density (in particular, tropospheric H_2O and stratospheric O_3),
- and where the temperature gradient is non-zero (temperature differences tend to zero in the AFGL 6 isothermal layer (levels 14-22)),
- and where the layering is coarse.

In this context, the differences between H_2O and air density weighted layer average temperatures in the lower troposphere are smaller because the vertical discretisation is finer. Note also that when the AIRS layering definitions are used, the differences between Curtis Godson absorber weighted and air density weighted layer average temperatures are less than 0.05 K for all layers.

The effect of the layer average temperature differences on the outgoing longwave radiation clearly depends on the wavenumber/weighting function. In particular, the layer average temperature differences illustrated here are expected to give rise to a cold bias in RTIASI brightness temperatures (compared to an equivalent 43 level GENLN2 calculation) in the 6.7 μm band, and the magnitude of the bias is expected to depend on atmospheric conditions.

Note that the effects of the 43 level vertical discretisation and the definition of layer average temperature are expected to compensate one another to an extent in the RTIASI fast model, but this does raise the question as to whether the 43 level Jacobians are consistent with equivalent calculations at higher vertical resolution.

Figure 8(b) illustrates the results of an equivalent comparison for the RTTOV arithmetic mean temperature difference (for the 43 RTIASI levels). In addition to the features observed previously, large differences are observed at the stratopause and to a lesser extent, the tropical tropopause. For the simulation of IASI observations, where

a significant number of channel radiances are influenced by CO_2 absorption in the upper stratosphere the air density weighted layer average temperature definition is a significant improvement on the arithmetic mean layer temperature.

3.1.5 Instrumental parameters

Despite an apparently clear definition of the level 1C radiances, apodisation was performed using a Maximum Optical Path Difference of 2.074 cm, and a corresponding Gaussian FWHM of 0.482 (the FWHM scales as 1/L)when generating the PFAAST fast model transmittance predictor scheme. KCARTA spectra have been convolved with the level 1C and PFAAST instrument spectral response functions and compared for six spanning atmospheres. In Figure 9 the median brightness temperature difference for the six atmospheres is traced as a function of channel wavenumber. There are significant differences thoroughout the spectral interval of interest, with largest sensitivity to apodisation changes in the 720 cm^{-1} Q branch, in the N_2O ν_1 and ν_3 bands ($\sim$ 1300 and 2220 cm^{-1} respectively). Note also that the corresponding channel variance (not illustrated here) is lower than the median brightness temperature difference - ie. the apodisation differences give rise to biases whose sign and the magnitude depend on wavenumber. In the intercomparisons which follow, KCARTA has been resampled and apodised in accordance with the PFAAST transmittance calculations.

3.1.6 Input profile uncertainties

Before concluding this section it is worth noting two additional sources of fast model error which proved important in initial intercomparisons:

- errors due to differences in interpolation of initial profile data onto fast model levels and
- errors due to differences in the vertical profile of N_2O (nominally a fixed gas).

As run to date[6], the layering preprocessing routine to GENLN2 performs a log-log interpolation of absorber number density (parts by volume) as a function of pressure. This is in contrast to the linear-log variation of absorber number density with pressure assumed in the KCARTA/PFAAST KLAYERS preprocessing routine and assumed when interpolating initial profile variables onto RTIASI or AIRS levels. The effect of differences in interpolation give rise to a $\leq$ 1% variation in absorber layer abundances. Specifically, for the 43 level atmosphere the log-log interpolation gives vapour layer abundances in the mid and upper troposphere which are 1% less than those calculated using a linear-log interpolation.

The impact of these differences was simulated using the RTIASI tangent linear code: these interpolation differences give correlated brightness temperature changes across the window region and the H_2O ν_2 band. The brightness temperature change remains less than 0.1 K throughout the spectral intervals in question for all of the six AFGL atmospheres tested. The median brightness temperature change was $\leq$ 0.05 K in the window region and $\leq$ 0.075 K in the ν_2 band.

In the simulations which will be discussed in the following sections, the initial profile was interpolated onto the fast model levels using a linear-log interpolation. This interpolated profile was then input to both fast model and line-by-line codes, thus eliminating interpolation errors.

The climatological variations of N_2O abundance and vertical distribution can give rise to brightness temperature changes of up to 0.5 K in the ν_1 and ν_3 N_2O bands. Clearly, errors of this magnitude will significantly modify the information content of channels in these spectral intervals. The climatological variations of N_2O should be taken into account when defining the forward model error covariance matrix. If brightness temperature changes due to the natural variability of other fixed gases and/or unmodelled atmospheric absorbers are of a comparable order of magnitude then these errors will also need to be reflected in the forward model error covariance matrix.

3.2 Conclusions and definition of a framework for intercomparison

In this section the characteristic magnitudes of the errors and error correlations associated with differences in spectroscopic parameters, modelled fixed gases, interpolation, discretisation of the radiative transfer equation, and modelled instrumental parameters have been discussed and illustrated. These errors are often comparable or greater than transmittance errors alone and should be taken into account, as appropriate, when specifying the forward model error covariance matrix. With regard to the latter two sources of error (specifically RTIASI vertical resolution and the PFAAST ISRF), where forward model errors and/or the degree of error correlation compromise the information content retrievable from observations the fast model should be modified. The specification and assessment of the impact of a non-diagonal forward model error covariance matrix on IASI retrievals is the subject of ongoing study.

[6]and clearly this can be modified if necessary - unfortunately appreciation of this particular problem came quite late on in the intercomparison.

Clearly a decision has to be made as to how to proceed in order to intercompare fast forward models. The intercomparison presented here is based on the following reasoning: the fast model intercomparison aims to assess the accuracy of modelled Level 1C radiances $\equiv$ the convolution of an 'infinite resolution' monochromatic spectrum with the instrument spectral response function. Atmospheric state, spectroscopic and instrumental parameters are taken as fixed, ie. as defined for fast model generation, but the simulation of the 'infinite resolution' spectrum should be optimal. Fast model radiance simulations are compared with equivalent line-by-line calculations. Forward model errors are estimated and fast models are compared based on their forward model error characteristics.

To ensure that input parameters were strictly equivalent for the fast model and its generator the 'optimality' reference simulation was somewhat compromised: the generator was run with the forward model vertical discretisation (this is also the vertical discretisation used for the Jacobian intercomparisons presented in Section 5). However wherever possible the sensitivity of results (forward model error) to RTE discretisation will be detailed.

Out of necessity, this first fast model intercomparison study has mainly focused on identifying the reasons for fast model errors which are much larger than published transmittance errors. In a second phase

- the optimal vertical and spectral resolution for high resolution simulations (with an associated measure of accuracy),
- a unique reference interpolation procedure,
- reference 'fixed' gas profiles and their climatological variability
- and optimal spectroscopic and instrumental parameters and uncertainties

will be defined, and a set of reference level 1C radiances generated in order to estimate the forward model error covariance matrix[7].

Because spectroscopy is taken to be fixed in these intercomparisons, KCARTA cannot be used to validate RTIASI. The use of KCARTA for fast model development is still an open question. There are real gains in speed for forward radiative transfer and Jacobian calculations. These are real considerations if a large data set is to be processed in order to estimate the forward model errors. The major disadvantages of KCARTA are the fixed vertical grid and the fixed spectroscopy. The 100 layer definition is probably more than adequate in terms of accuracy of the radiative transfer calculations, but the fixed layering is less convenient if fast model errors are to be diagnosed and physical quantities are required on different pressure levels. Similarly, the KCARTA spectral resolution is probably adequate for all practical purposes, with the possible exception of the 15 μm band centre, however the inflexibility of the kcompressed database is a real handicap. The validity of the choice of H_2O spectroscopic parameters can only be confirmed (or otherwise) via comparison with observations. In the interim, it would seem important to also have access to standard, documented databases: kcompressed versions of the most recent HITRAN and GEISA databases for example. Note also that model output should be subject to testing to ensure validity - this is not a criticism of KCARTA specifically, as GENLN2 output also required validation.

A final point on the question of documentation - a lot of time was spent tracking down detail of the fast model implementation, and to a lesser degree, detail of the reference model implementation - 'detail' which nevertheless gave rise to significant brightness temperature differences. Adequate accompanying documentation should (almost) be a requirement/criteria for fast model selection !

[7] In the short term a single input profile interpolation scheme will be chosen and high vertical resolution GENLN2 simulations will be rerun with the current uncertainties introduced by differences in interpolation of the input profiles eliminated.

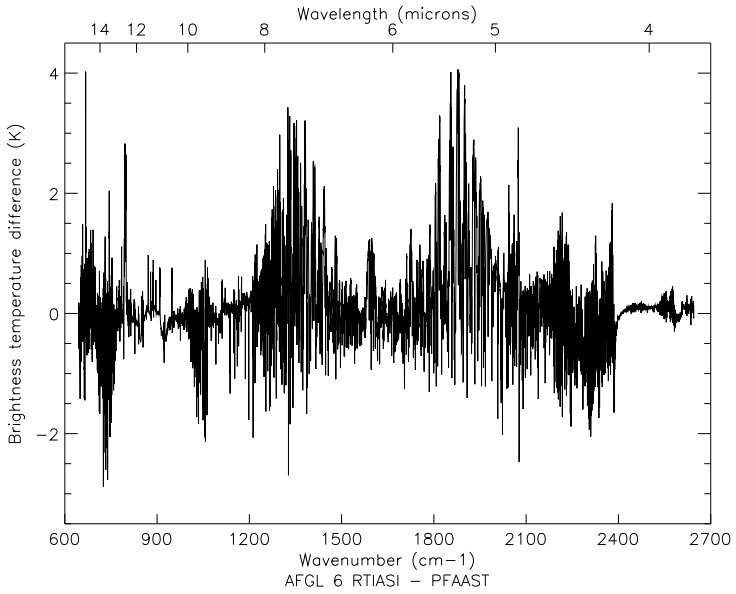

Figure 3: Direct intercomparison of the brightness temperatures simulated by RTIASI and PFAAST for the AFGL U.S. Standard Atmosphere. The difference in brightness temperature (RTIASI-PFAAST) is illustrated as a function of wavenumber and wavelength.

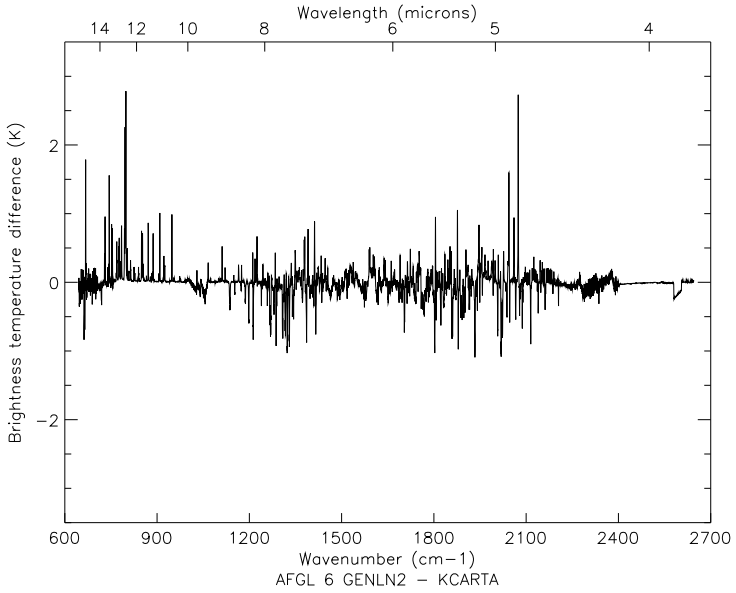

Figure 4: Intercomparison between GENLN2 and KCARTA simulations of IASI level 1C radiances (brightness temperatures) for the AFGL U.S. Standard atmosphere. The large differences ($\geq \pm$ 0.5K) in simulated brightness temperatures are related to differences in the spectroscopic parameters used for some water vapour lines.

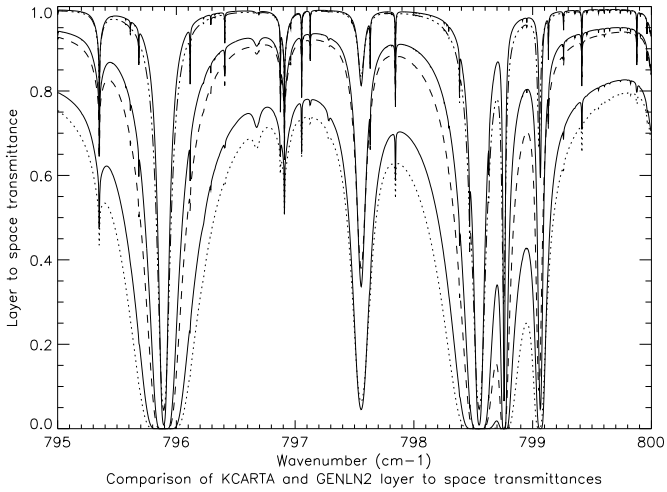

	HITRAN96			TOTH		
wavenumber	S	γ_{air}	γ_{self}	S	γ_{air}	γ_{self}
795.8936	1.680E-22	0.0432	0.0000	1.680E-22	0.0668	0.3800
797.5554	1.670E-23	0.0556	0.0000	1.670E-23	0.0652	0.3100
798.5495	1.520E-22	0.0457	0.0000	1.520E-22	0.0727	0.3800
798.7563	6.420E-23	0.0109	0.0000	6.420E-22	0.0269	0.2260
799.0536	2.140E-23	0.0198	0.0000	2.140E-23	0.0269	0.1720

Figure 5: Illustration of the impact of differences in modelled spectroscopic parameters. GENLN2 and KCARTA use different water vapour halfwidths in the 795 to 800 cm^{-1} interval. Halfwidths γ (cm^{-1}/atm) are tabulated for the strongest water vapour lines in this interval. Layer to space water vapour transmittances are illustrated for three levels in the atmosphere (lower stratosphere, upper troposphere and lower troposphere). In each case GENLN2 transmittances are given by a solid line and KCARTA transmittances are given by a broken line (dot dashed=LS, dashed=UT, dotted=LT). Layer to space transmittances can differ by up to 5%, resulting in significant differences in simulated brightness temperatures.

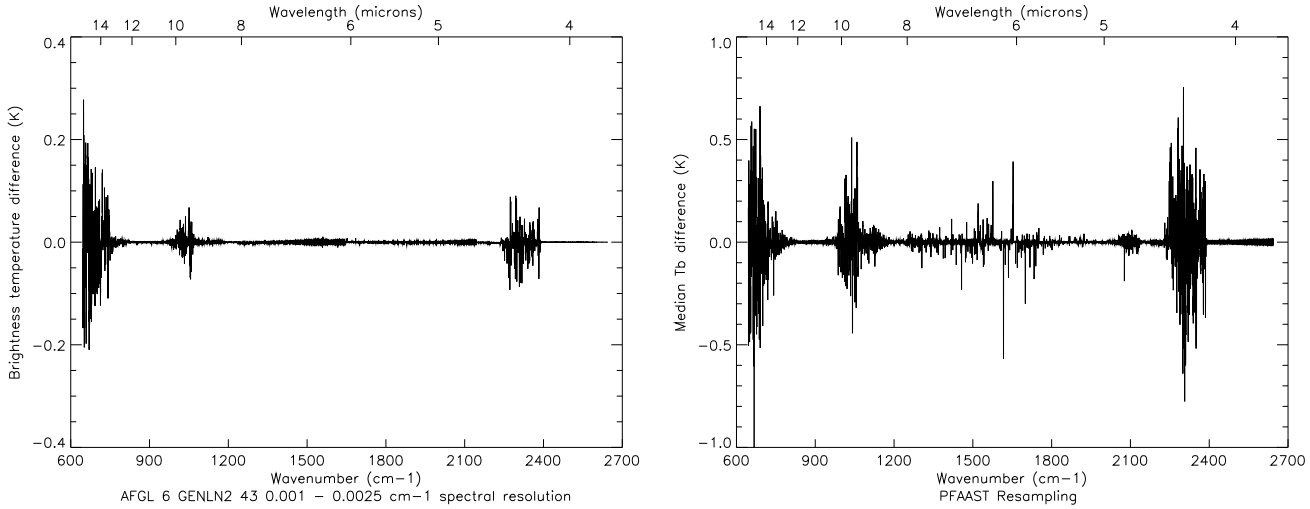

(a) (b)

Figure 6: Impact of the spectral resolution used when simulating the high resolution radiance spectra on the resulting level 1C radiances: (a) characteristic brightness temperature changes when changing the spectral resolution of high resolution radiance calculations from 0.001 to 0.0025 cm^{-1}, (b) median of the brightness temperature change when KCARTA high resolution spectra are resampled at the PFAAST generator resolution before convolution with the ISRF.

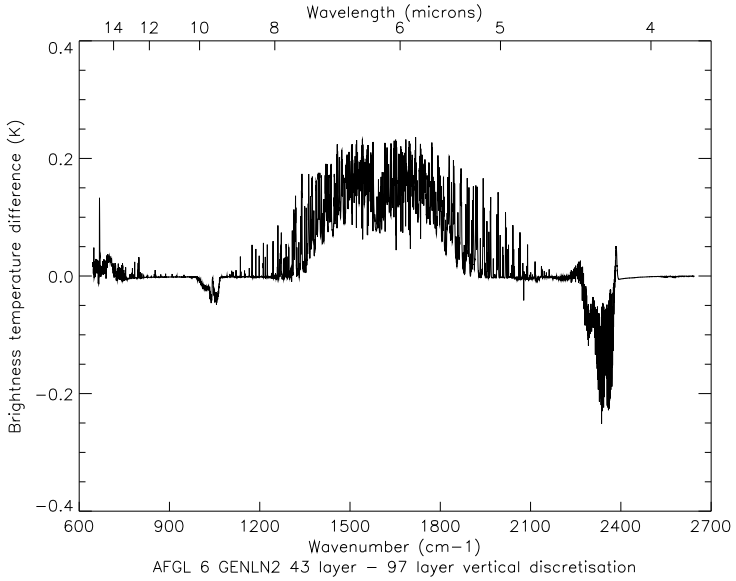

Figure 7: Differences in level 1C radiances simulated by GENLN2 using the two fast model definitions (43 level RTIASI and 101 (97) level AIRS/PFAAST) layering definitions for the AFGL U.S. Standard atmosphere.

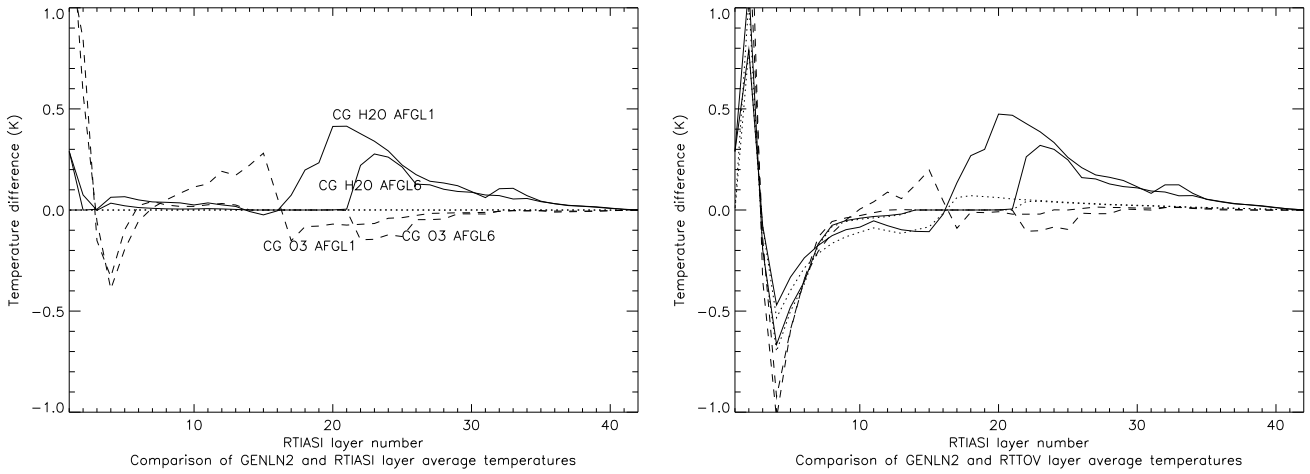

(a) Comparison with air density weighted layer average temperatures

(b) Comparison with RTTOV layer average temperatures

Figure 8: Differences between Curtis Godson absorber weighted layer average temperatures and (a) air density weighted layer average temperatures and (b) RTTOV layer average temperatures. Differences are illustrated for two atmospheres (AFGL1 (tropical) and AFGL6 (U.S. Standard)) and three absorbing gases H_2O (solid line), CO_2 (dotted line) and O_3 (dashed line) as a function of RTIASI layer number. Layer 1 extends from 0.29 to 0.1 mb, layer 42 extends from 1005.42 to 1013.0 mb.

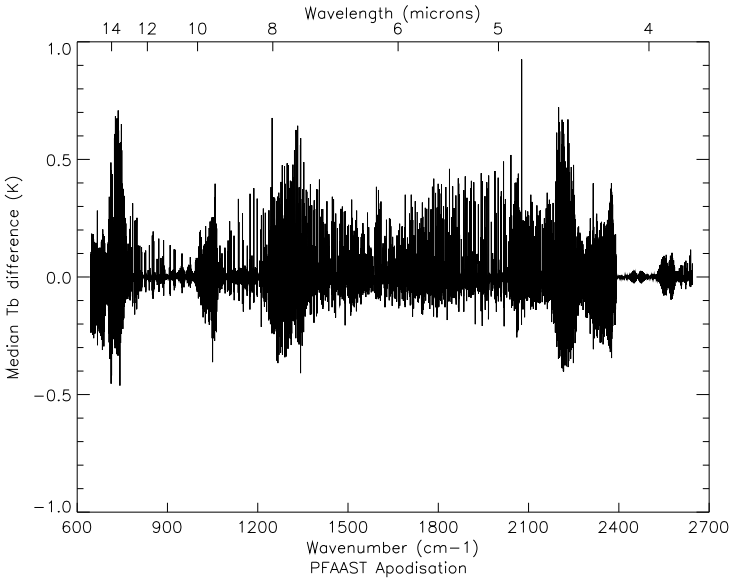

Figure 9: Illustration of the effects of differences in the modelled ISRF. KCARTA spectra have been apodised using two ISRF definitions (MAX OPD equal to 2.0 and 2.074 cm) and the resulting brightness temperature differences have been evaluated for six different atmospheres. The median of brightness temperature differences arising from differences in the modelled IASI instrument spectral response function are illustrated here.

4 Intercomparison of Fast model/Generator differences

In this section we consider the differences in the simulated level 1C radiances when each fast model is compared with its generator for an ensemble of six independent[8] atmospheres. The atmospheres selected represent (to a reasonable degree) the seasonal and latitudinal variations of temperature, water vapour and ozone. The intercomparison is restricted to clear sky radiances, simulated for a nadir viewing geometry and a surface emissivity of 1.0 (a perfectly absorbing lower boundary).

Because the test sample size is so small robust statistics, the median, the fourths and the fourth spread d_F, are used to summarize the essential features of the level 1C radiance differences. The median and fourths are order statistics (letter summaries). The N observations (realisations) are ordered in increasing (or decreasing) magnitude of the measured quantity, the brightness temperature difference in this case. The depth of a particular value is given by the Min(upward rank,downward rank). The median is the value whose depth is $(N+1)/2$. If N is even then the median is given by the arithmetic mean of x_k and x_{k+1}, where $N = 2k$. The depth of the fourths is given by (depth of median + 1)/2. Upper and lower fourths F_U and F_L, are extracted with interpolation as above if necessary. The fourth spread d_F, is given by $F_U - F_L$.

These statistics give a robust and efficient summary of features a larger sample size is expected to exhibit if the small sample set is representative. If errors have a Gaussian distribution then the median and mean are equivalent and the fourth spread is equal to 1.549σ. This gives rise to the notion of a pseudo standard deviation $d_F/1.549$. Note finally non-zero median brightness temperatures will be discussed in terms of bias, but in some cases reflect errors which depend on atmospheric state. Correlation coefficients are not illustrated, but correlation of errors on ~ 100 cm^{-1} intervals is commented where significant.

Median, fourth spread and root mean square level 1C brightness temperature differences are illustrated as a function of wavelength (wavenumber) in Figures 10, 11 and 12. RTIASI is compared with GENLN2 using air density and Curtis Godson absorber weighted layer average temperature in the GENLN2 radiative transfer calculations in Figures 10 and 11 respectively. PFAAST is compared with KCARTA in Figure 12.

The major signatures and/or characteristics of the fast model errors may be summarized as follows:

- In the **15 μm CO_2 band centre** RTIASI has a lower RMS error than PFAAST. RTIASI has lower bias and lower or comparable variance. For both models the level 1C RMS errors are significantly larger than the transmittance errors alone.

- In the **700 - 800 cm^{-1} region** RTIASI has a higher RMS error than PFAAST. Bias and variance make approximately equal contributions to the RMS error for both models. Errors are comparable with transmittance errors.

- In the **window region (8 - 12 μm)** both components of the RTIASI RMS error are larger than the corresponding PFAAST components. RTIASI errors are largest for the humid atmospheres and have a high degree of correlation across the spectral interval. The only significant PFAAST errors occur at H_2O line centres.

- In the ν_1 and ν_3 **Ozone bands** performance of both models is relatively poor. RMS errors are typically between 0.2 and 0.4 K - ie. of the same magnitude as instrumental noise. Bias and variance components of the RMS error are comparable for both models.

- In the **H_2O ν_2 band** RTIASI presents large errors with a high degree of correlation across the band. Bias and variance are reduced when layer average temperature effects are removed (ie. comparison with GENLN2 calculations using the CO_2 path average temperatures in the radiative transfer calculations), but even in this case RTIASI errors are larger than PFAAST errors and exhibit state dependence.

- In the 4.3 μm CO_2 band centre forward model errors are much greater than transmittance errors alone. The models differ in the relative magnitude of bias and variance: PFAAST has high bias and low variance, RTIASI has higher variance, although bias does make a significant contribution to the RMS errors[9]. However, given the magnitude of spectroscopic errors in the 4.3 μm band centre, these forward model errors not of particular concern in themselves. In the **2150-2300 cm^{-1} interval** the errors from both models are less than or of the order of 0.1 K.

However, these graphical representations tend to overemphasize the largest errors and do not illustrate much of the information which is of interest for assimilation and channel selection - the number of channels with low RMS error and/or the error characteristics for channels between lines (where weighting functions are narrower) in

[8]Independent of the profile set used to generate the fast models regression coefficients.

[9]The source of these differences is not currently well understood - the effect of differences in apodisation routines has been checked - brightness temperature differences remain less than 0.15 K in this interval (the maximum error on the entire IASI spectral interval in fact - with few exceptions elsewhere errors are less than 0.05 K).

wavenumber intervals susceptible to provide useful sounding information, for example. For this reason errors and screening statistics for the HIRS channels are illustrated below.

4.1 Detailed intercomparison for the HIRS channels

In Figures 13 and 14 the median and upper and lower fourths are plotted for wavenumber intervals corresponding to HIRS sounding channels. Screening statistics for the two fast models are summarised in Table 2: on the spectral intervals spanned by each of the HIRS channels the percentage of IASI channels with forward model RMS errors and/or pseudo standard deviations of less than 0.1 and 0.2 K are tabulated. As an indication of the sensitivity of the screening statistics to the detail of the treatment of the RTE two sets of values are given, where relevant, for each fast model. Thus, RTIASI screening statistics are given for comparison with GENLN2 calculations using Curtis Godson absorber weighted temperatures. Screening statistics for equivalent calculations using air density weighted layer average temperatures are given in parentheses. Similarly, PFAAST screening statistics are given for comparison with KCARTA calculations using the PFAAST apodisation parameters, but without resampling. The equivalent statistics for resampled KCARTA spectra are given in parentheses and in the figures illustrating IASI fast model errors in the HIRS channels.

From these graphs and the tabulated screening statistics it is apparant that with the exception of HIRS channels 1,2,3,4 and 9 (PFAAST) and HIRS channel 12 (RTIASI) more than 75% of channels have forward model RMS errors of less than 0.2 K. Similarly in all but HIRS channels 1 and 9 (PFAAST) and HIRS channels 9, 12 and 16 (RTIASI) more than 75% of channels have forward model pseudo standard deviations of less than 0.1 K. The low variances (pseudo standard deviations) imply that the fast model Jacobians should be reasonably accurate: for example, if forward model errors only vary by ~ 0.1K for temperature variations of tens of degrees, then one would expect the effects of small temperature perturbations to also be well reproduced. Note also that with exception if 15 μm band centre ($\nu < 760$ cm^{-1}) the maximum errors occur for both models in the centres of strongly absorbed lines.

Differences between the screening statistics based on the RMS error and the pseudo standard deviation are indicative of non-zero mean brightness temperature differences. Bias makes a significant contribution to the PFAAST RMS error in HIRS channels 1 to 7 and the screening statistics are strongly influenced by resampling. Bias has a significant impact on screening statistics for RTIASI in HIRS channels 4 to 7 (where water vapour absorption begins to make significant contributions to transmittances) and in channels 11, 12 and 16. Given the importance of intervals affected by bias, in terms of potential information for sounding, it is of interest to identify the origin of the biases in question.

It should be clear from the results considered here and in subsection 3.1.4 that much of the bias in H_2O ν_2 band brightness temperatures simulated by RTIASI is due to differences in the layer average temperatures used in the radiative transfer calculations. These differences arise because the the vertical discretisation of the upper troposphere in the 43 level model is relatively coarse; coarse enough for the assumptions regarding the average temperature of the absorbing gas in the layer (ie. assumptions regarding the vertical variation of absorbers (and temperature) within the layer) to give rise to significant differences in the layer average temperature and ultimately, the simulated outgoing radiation.

A modification to the layer average temperature calculation[10] could be envisaged for radiative transfer calculations in spectral intervals where water vapour is the principal absorbing gas. If the results (forward model errors) obtained with this modification were comparable with the RMS and pseudo standard deviation for the GENLN2 air density weighted intercomparisons, this might be deemed an adequate solution to what must otherwise be viewed as an unacceptable level of forward model error and error correlation. However, given partial compensation of errors due to vertical discretisation and layer average temperature definitions suggested by the results described in subsection 3.1.4, it will be necessary to rerun GENLN2 calculations with the AIRS vertical layering (or a similar optimal vertical discretisation) but eliminating interpolation errors before conluding on the merits of such a modification to the layer average temperature. Note also that in the real atmosphere the H_2O number density is not always a monotonic decreasing function of height. Any decisions regarding the definition of layer average temperature and the attribution of forward model error should also take into account the associated representativity errors, and these will be influenced by the choice of vertical layering.

Even when layer average temperature effects are taken into account (eg. GENLN2 simulations using air density weighted layer average temperatures), RTIASI has higher variance than PFAAST in the the ν_2 band and in the window region ($\lambda > 12\mu$m). Forward model errors are larger for atmospheres with high water vapour contents in both these spectral regions. The test cases are not extreme, so this feature probably reflects a real problem with the RTIASI water vapour predictor scheme. Specifically, the profile set used to determine the regression coefficients contains an (arguably) disproportionate number of dry water vapour profiles. In this case, it is not inconceivable that the regression relations are less accurate for atmospheres with high water vapour contents. Higher errors

[10]By replacing the air density by the water vapour number density $\equiv q(z).n(z)$ in the Curtis Godson layer average temperature calculation, for example.

in humid atmospheres were also found by M. Matricardi when determining RTIASI transmission errors on an independent profile set. It is hoped that the upcoming ISSWG fast model intercomparison study will provide further elements of response to this question, and identify modifications to the water vapour predictor scheme if these are required. In this context, note that PFAAST uses a separate continuum predictor scheme ie. convolved transmittances for lines and for continuum absorption are predicted separately and then summed.

The origin of the high bias in PFAAST forward model errors in the 15 μm band centre is not fully established, but is believed to be associated with the spectral resolution used to generate the forward model: of all the sensitivity tests performed, only resampling gives rise to biases of the order of magnitude observed in both the 15 and 4.3 μm CO_2 band centres. The error (bias) characteristics are improved, but not eliminated when the KCARTA spectra are resampled - however this may be due to the resampling of the high resolution radiances as opposed to the high resolution transmittances. Differences in the detail of the Fast Fourier Transform and apodisation routines are not expected to give rise to bias of this order of magnitude. Two FFT/apodisation routines have been compared giving brightness temperature differences of less than 0.05 K throughout this spectral interval. The Matlab routine used to apodise the PFAAST transmittance data has not been tested however. Similarly, the errors which may arise from the linear interpolation of the (oversampled) apodised spectrum (KCARTA/PFAAST simulations only) are estimated to be $\leq$0.03 K - ie. an order of magnitude less than the observed biases. It is possible that the differences in the fast model error characteristics are related to differences in the temperature profiles of the two independent sets. In particular, the six TIGR temperature profiles used in the PFAAST/KCARTA simulations generally have a well defined tropopause and more structure in the lower stratosphere than the AFGL atmospheres.

Both models show a marked increase in variance, as compared with transmittance errors alone, in the 15 μm band and the largest errors for both models occur in strongly absorbed 15 μm band centre and 720 cm^{-1} CO_2 Q branch. This may be indicative of a breakdown of the polychromatic approximation (and would explain the high degree of sensitivity to spectral resolution in this spectral interval). This has not been tested explicitly. The differences in apodisation routines mentioned above may also account for part of the increased variance. Note finally that the error characteristics and screening statistics for RTIASI in the CO_2 bands are not significantly modified when compared with GENLN2 simulations using the AIRS vertical layering definition (although again this may be a reflection of the temperature gradients/structures of the AFGL set).

In summary, overall there are a more than sufficient number of channels with forward model errors (variance) which are significantly lower than instrumental noise. There is evidence for a problem with the modelling of H_2O absorption in RTIASI - correlated, atmospheric state dependent errors are the dominant signature in the window ($\lambda < 12$ μm) and the H_2O ν_2 band. The impact of these correlated errors on retrievals will need to be assessed, and error characteristics may need to be improved if RTIASI is to be adopted for NWP development. The adequacy of the 43 level vertical discretistion remains an open question. In practice, if this layering is retained it will probably be necessary to specify a higher forward model error in the H_2O ν_2 band to account for discretisation and representativity errors.

PFAAST performance is generally satisfactory and even preferable at wavelengths less than 12μm: the choice of spectral resolution (for fast model generation) does appear to degrade the model performance in the 12 to 15 μm interval. The differences between the modelled and Level 1C instrument spectral response functions give rise to brightness temperature differences which are significantly larger than the HIRS band error characteristics illustrated here (recall Figure 9). Errors of this order of magnitude would compromise the effective information content of the IASI measurements if the current version of the PFAAST model was used to assimilate level 1C radiances. Results would suggest that with re-apodisation (without resampling) and regeneration of fast model regression coefficients the PFAAST fast model formulation would give very satisfactory Level 1C radiance estimates.

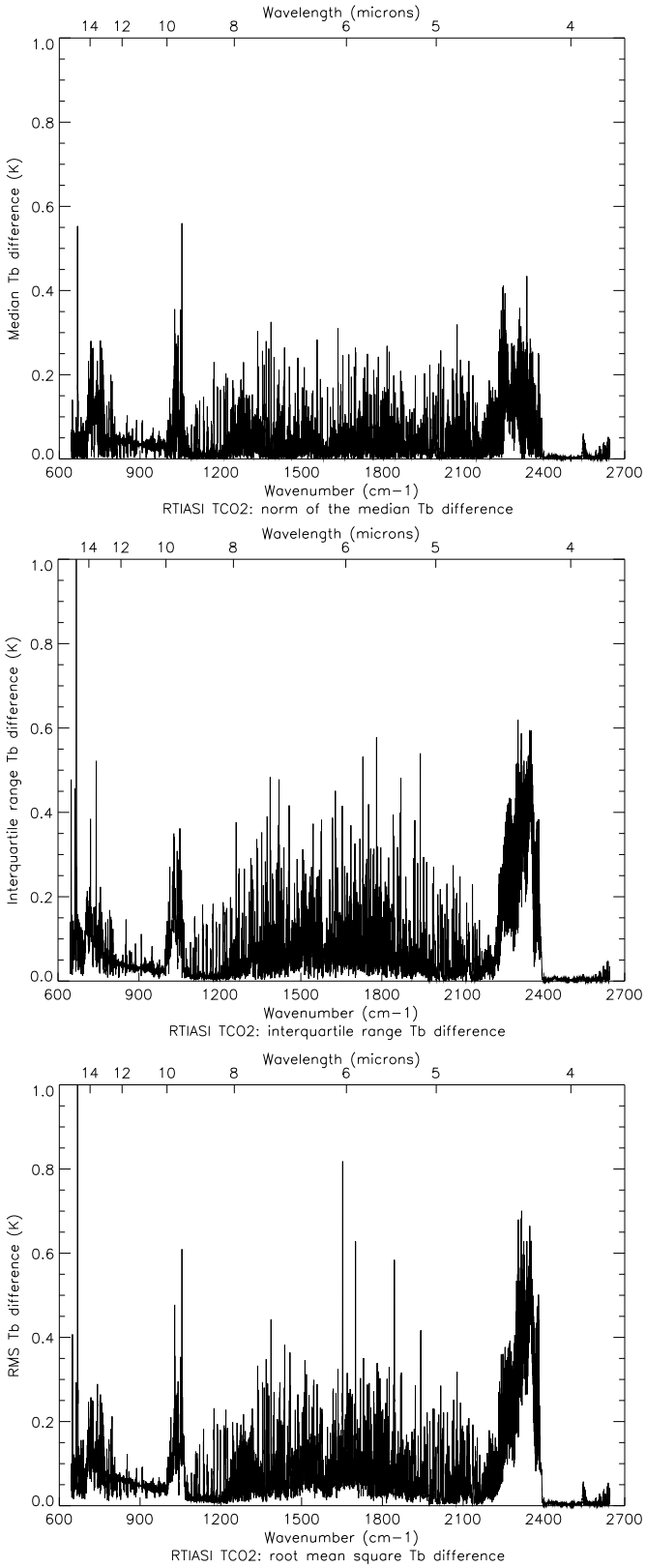

Figure 10: From top to bottom: median (norm), fourth spread and root mean square brightness temperature differences for RTIASI when compared with GENLN2 level 1C radiance simulations using air density weighted layer average temperatures (CO_2 path average temperatures) for the radiative transfer calculations.

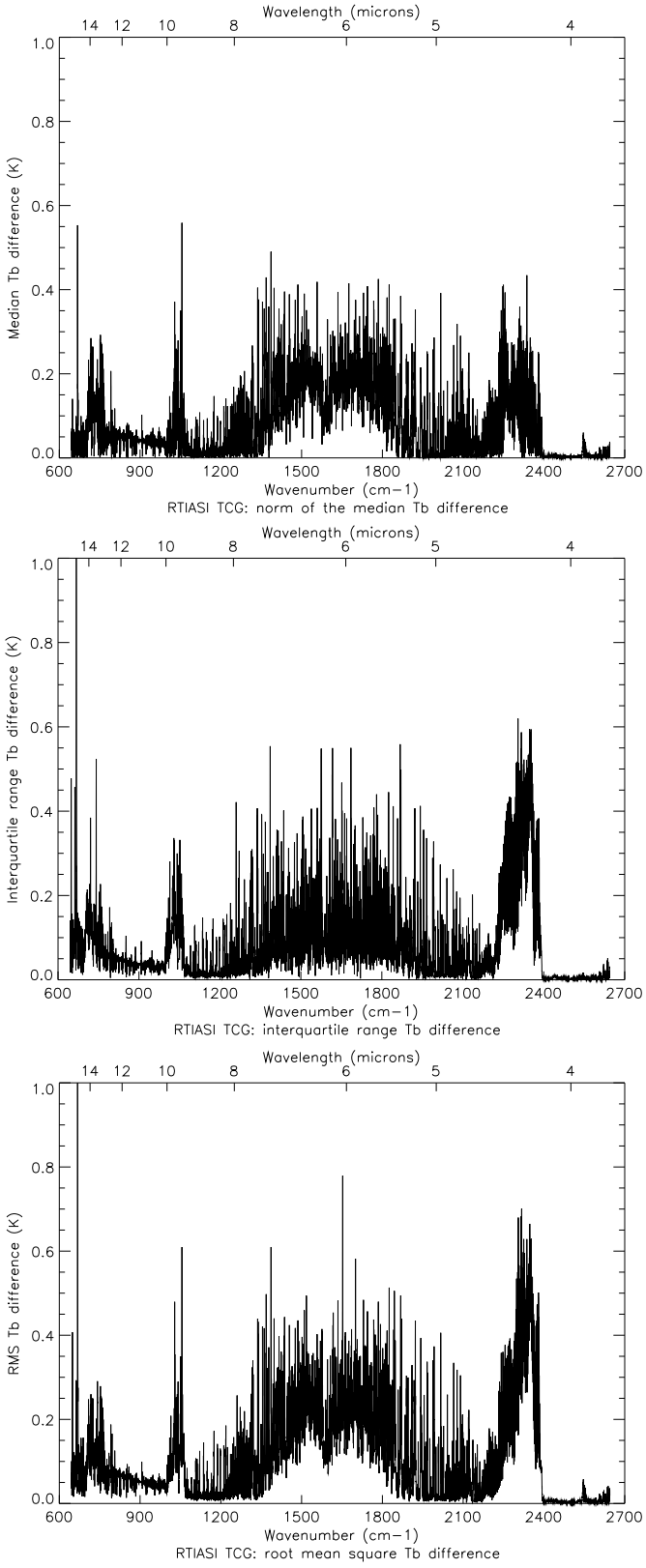

Figure 11: From top to bottom: median (norm), fourth spread and root mean square brightness temperature differences for RTIASI when compared with GENLN2 level 1C radiance simulations using Curtis Godson absorber weighted layer average temperatures for the radiative transfer calculations.

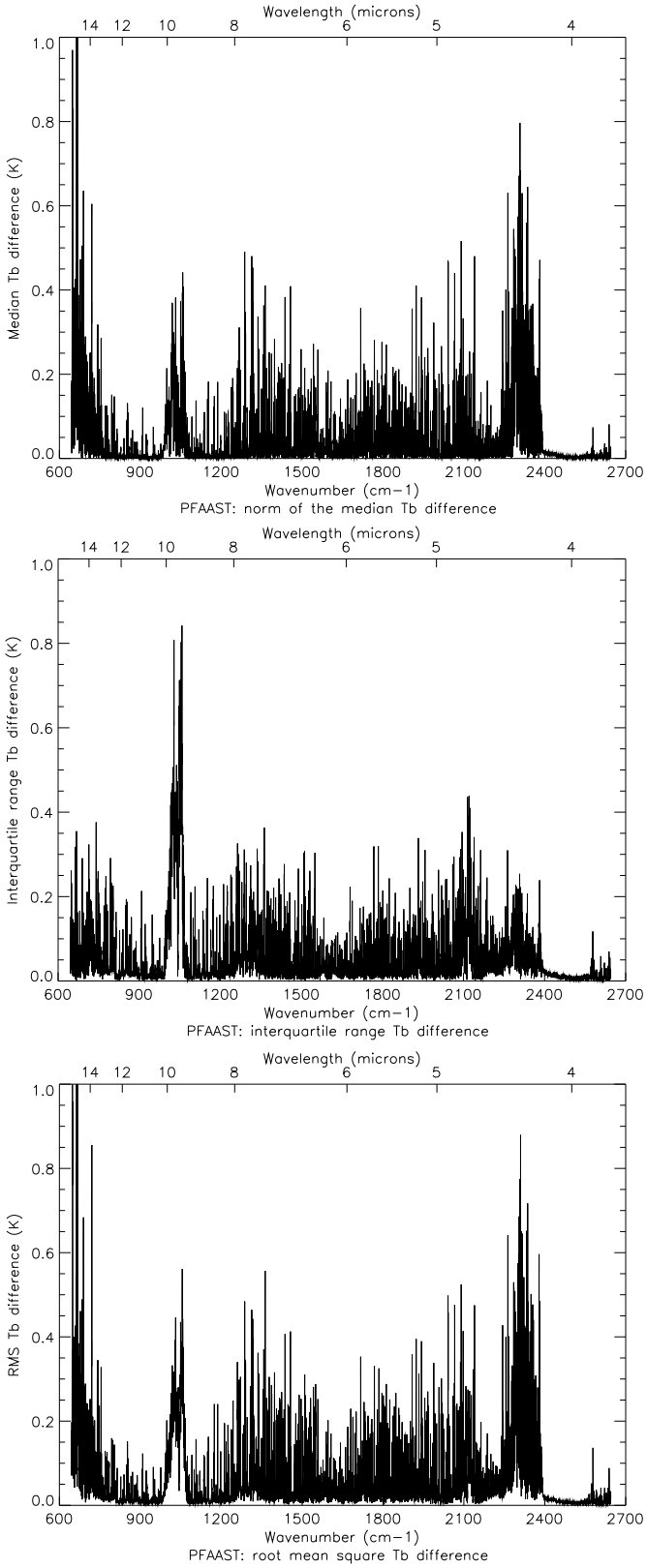

Figure 12: From top to bottom: median (norm), fourth spread and root mean square brightness temperature differences for PFAAST when compared with KCARTA radiance simulations. KCARTA radiances were apodised with the same instrument parameters as those used to generate the PFAAST fast model. Both models use air density weighted layer average temperatures for the radiative transfer calculations.

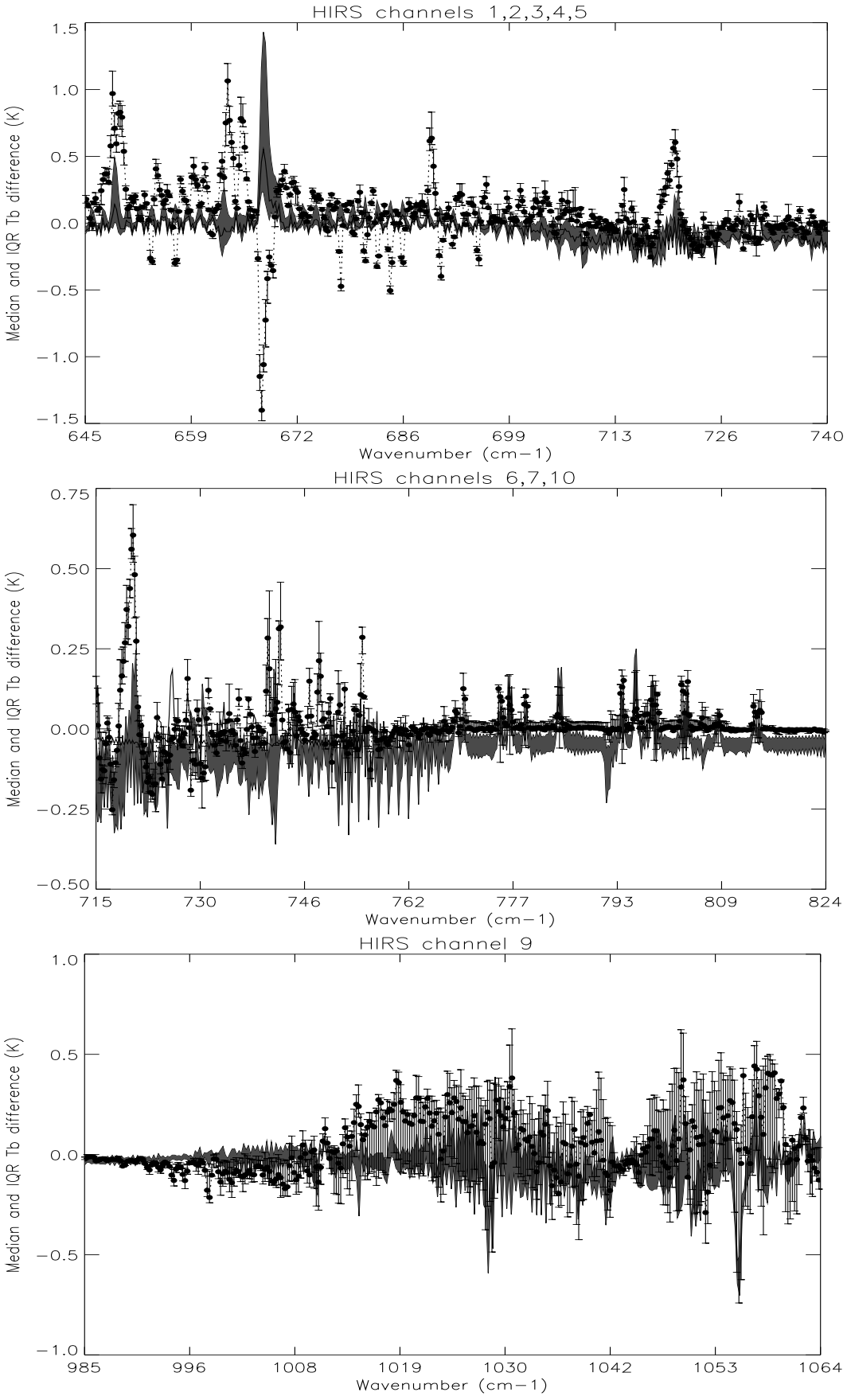

Figure 13: Median and upper and lower fourths plotted for PFAAST (dots and errorbars) and RTIASI (coloured zones (delimited by lower and upper fourths) for channels in the spectral intervals spanned (from top to bottom) by HIRS channels 1 to 5, 6, 7 and 10 and HIRS channel 9 (see Table 2 for details of the wavenumber intervals for individual channels).

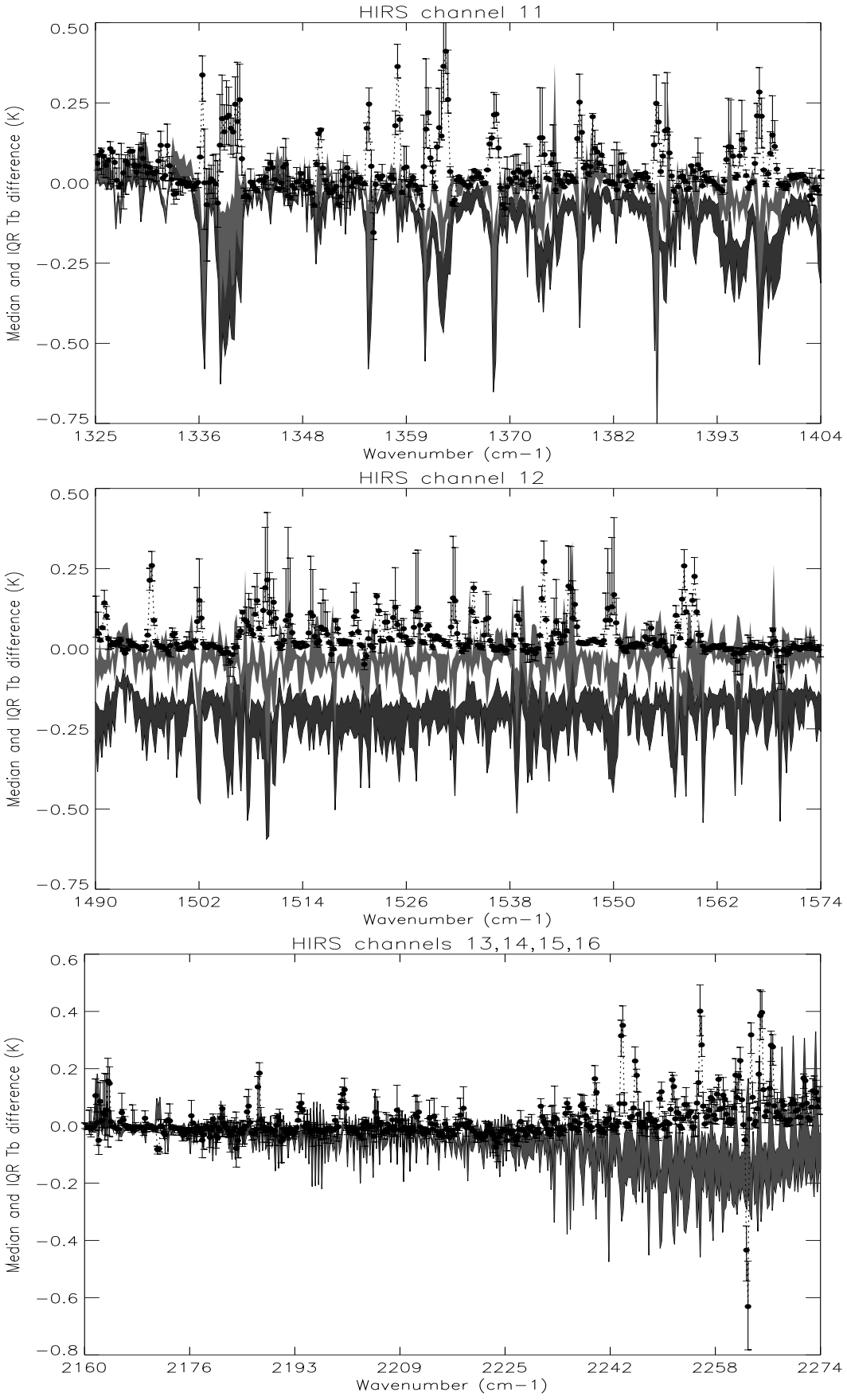

Figure 14: Median and upper and lower fourths plotted for PFAAST (dots and errorbars) and RTIASI (coloured zones (delimited by lower and upper fourths) for channels in the spectral intervals spanned (from top to bottom) by HIRS channel 11, 12 and HIRS channels 13 to 16 (see Table 2 for details of the wavenumber intervals for individual channels).

HIRS channel number and wavenumber interval	% of channels with RMSE≤0.1K and/or d_F ≤0.155K				% of channels with RMSE≤0.2K and/or d_F ≤0.3K			
	RTIASI		PFAAST		RTIASI		PFAAST	
	RMS	d_F	RMS	d_F	RMS	d_F	RMS	d_F
1: 660-680 cm^{-1}	62	77	10 (22)	72 (87)	84	88	28 (46)	94 (98)
2: 660-695 cm^{-1}	72	86	15 (30)	82 (88)	91	93	41 (56)	97 (99)
3: 670-710 cm^{-1}	75	89	22 (43)	90 (93)	98	100	61 (74)	100
4: 680-725 cm^{-1}	56	78	26 (48)	87 (90)	90	99	71 (80)	99
5: 690-740 cm^{-1}	44 (46)	77 (80)	36 (57)	88 (93)	90 (91)	99	82 (88)	99
6: 710-755 cm^{-1}	33 (37)	81 (82)	48 (61)	85 (89)	87 (88)	98	90	99
7: 720-770 cm^{-1}	40 (45)	88 (89)	64 (73)	91 (92)	90 (97)	98	94	99
8: 850-940 cm^{-1}	100	100	99	99				
9: 985-1065 cm^{-1}	56 (53)	72 (72)	25	35	93	99	57	57
10: 780-820 cm^{-1}	94 (93)	99 (99)	90	91	100	100	100	100
11: 1325-1405 cm^{-1}	54 (79)	85 (90)	77	89	78 (93)	97	89	99
12: 1490-1575 cm^{-1}	03 (60)	74 (87)	82	95	30 (96)	97	94	99
13: 2160-2220 cm^{-1}	90	100	95	97	100	100	100	100
14: 2180-2240 cm^{-1}	81	96	97	98	98	100	100	100
15: 2205-2230 cm^{-1}	83	100	99	99	100	100	100	100
16: 2210-2275 cm^{-1}	38	62	74 (84)	99	77	92	88 (95)	100
17: 2385-2450 cm^{-1}	97	100	99	100				
18: 2475-2565 cm^{-1}	100	100	100	100				

Table 2: Screening statistics of forward model errors for IASI channels in the spectral intervals spanned by the given HIRS channels. The percentage of channels with RMS errors and pseudo standard deviations less than 0.1 and 0.2 K are tabulated for the two fast models. The screening statistics for RTIASI when layer average temperature effects are eliminated are given in brackets where appropriate. Similarly, PFAAST screening statistics for comparison with resampled KCARTA spectra are given in brackets (although these are the values plotted in the HIRS graphs). Note that the RTIASI screening statistics in the CO_2 bands are not significantly modified when the fast model is compared with GENLN2 calculations performed with the AIRS layering.

5 Comparison of modelled Jacobians

In addition to providing an accurate forward radiative transfer model, fast Jacobian or adjoint calculations are required for direct radiance assimilation. Moreover, fast models will typically be used to evaluate the Jacobian matrix elements for channel selection studies because of the prohibitive computational cost of Jacobian calculations using line-by-line models. For these reasons, fast model temperature and water vapour Jacobians have been compared with the Jacobians calculated using each fast model generator on three spectral intervals for two[11] 'extreme' atmospheres; a hot/humid tropical atmosphere and a cold/dry sub-arctic winter atmosphere.

Brightness temperature perturbations calculated using the RTIASI tangent linear code have been compared with GENLN2 brute force calculations and PFAAST brute force calculations have been compared with analytic and brute force Jacobians from KCARTA. Note that tangent linear, adjoint and k codes are being developed by M. Matricardi for the RTIASI fast model. According to personal communication from L. Larrabee Strow, there is no plan for tangent linear or adjoint codes to be developed for PFAAST at UMBC. Clearly, given the use of variational data assimilation at the UKMO, this is a serious limitation for the PFAAST model.

In order to evaluate the Jacobian matrix elements, input profile variables were perturbed by +1K for the temperature Jacobian calculations and by a relative variation $\Delta\ln(q)$=-0.05 ie. a 5% reduction in the water vapour for each level/layer in turn for the water vapour Jacobian calculations. The magnitudes of these perturbations were based on the results from a previous study on the validity of the tangent linear hypothesis for ATOVS [13] and seek to ensure a linear response to profile perturbations.

Although every effort has been made to treat the pertubation calculations in the same manner between fast model and generator, the following differences should be noted:

- The specification of temperature perturbations on pressure levels gives rise to variations in both layer average temperature and gas density (and hence absorber abundance) in adjacent layers in the GENLN2 calculations (as compared with a simple temperature variation in RTIASI).
- Similarly, a perturbation in the water vapour content at a pressure level will affect both the water vapour content and layer average temperature in adjacent layers in the GENLN2 calculation (Curtis Godson absorber weighted layer average temperatures were used in the GENLN2 radiance calculations).
- KCARTA temperature Jacobians were simulated using the level 1C apodisation/ISRF definition and were not resampled.

The effects of departures from linearity and changes in layer average temperature have been quantified for the RTIASI/GENLN2 water vapour Jacobian intercomparisons and will be discussed below. The effects of density perturbations are expected to be small by comparison. Resampling and reapodisation of KCARTA spectra and re-evaluation of Jacobian elements has not been undertaken to date, mainly because a number of problems had to be resolved regarding the Jacobian calculations from the generating/reference models. Specifically, the Jacobians generated by GENLN2 using variable fine spectral grid (10 points per halfwidth) presented unphysical behaviour; finite, constant response to profile perturbations in layers far from the weighting function maximum. This problem is eliminated when calculations are performed on a fixed fine mesh grid. Problems were also found with the analytic gas density Jacobians from KCARTA, and reported to the developers at UMBC. This bug has now been corrected. At the time of writing the PFAAST study was not complete, but brute force water vapour Jacobians and analytic temperature Jacobians have been calculated using KCARTA for the hot/humid atmosphere (expected to be the more testing of the two cases) and those results are presented here, along with the equivalent GENLN2/RTIASI intercomparison.

In the following paragraphs we first compare the performance of PFAAST and RTIASI on three spectral intervals: 645-800 cm^{-1}, 885-915 cm^{-1} and 1300-1450 cm^{-1} for a tropical atmosphere. We then examine the RTIASI tangent linear water vapour Jacobians in more detail. Jacobian results obtained with the November 1999 RTIASI release are are discussed and Jacobians for the AFGL5 sub arctic winter atmosphere are presented. The implications of atmospheric state and spectroscopic dependencies are described.

5.1 Comparison of RTIASI and PFAAST Jacobians for the case of a humid atmosphere

Figure 15 illustrates the temperature Jacobians calculated by KCARTA for a tropical atmosphere in the 645 to 800 cm^{-1} interval. A cross-section through the surface for the IASI channel at 645.113 cm^{-1} is compared to the corresponding PFAAST brute force Jacobian (dashed line) in the lower graph. The agreement between the fast model and its generator is very satisfactory and is characteristic of the agreement obtained in a large number of

[11] Only one atmosphere has been studied for PFAAST, for reasons described below.

channels for both fast models. In order to summarize the fast model-generator Jacobian intercomparisons we will consider the maximum relative error

$$\mathrm{Max}\left|\frac{\Delta \mathrm{TB}_{\mathrm{ref}} - \Delta \mathrm{TB}_{\mathrm{fast}}}{\Delta \mathrm{TB}_{\mathrm{ref}}}\right|, \tag{4}$$

as a function of channel wavenumber. The maximum relative error (i) for levels where the change in brightness temperature is $\geq$ 0.5 MaxΔTB and (ii) for levels where the change in brightness temperature is $\geq$0.1 MaxΔTB will be illustrated with lines and dots respectively. Where the two measures are equal the maximum error for the given channel occurs in the region of the central maximum (either the magnitude, form or position of the central maximum[12]), otherwise the maximum error is associated with the description of the Jacobians for levels/layers of lower sensitivity (0.1 MaxΔTB $\leq \Delta$TB $\leq$ 0.5 MaxΔTB). For reference, the maximum errors for the channel illustrated are: (i) 2% (layer number 45) and (ii) 10% (layer number 80).

Fastmodel-generator temperature Jacobian intercomparisons for the 645 to 800 cm^{-1} and 1300 to 1450 cm^{-1} wavenumber intervals are presented in Figures 16 and 17 respectively. Temperature Jacobians in the 1300 to 1450 cm^{-1} interval are generally well described by both fast models: the maximum error in the central maximum is usually less than 5% and the overall error is usually less than 10%. Larger errors (10 to 20 (40) %) occur where there is strong absorption. Fast forward model errors are also largest for these channels.

In the 645 to 800 cm^{-1} wavenumber interval the fast models differ quite markedly in their performance, relative to their generators, although maximum errors still occur where forward model errors are greatest. In the 645 to 700 cm^{-1} interval RTIASI gives a good description of the temperature Jacobians: the error in the description of the central maximum is less than 2% throughout almost the entire interval, and overall errors are less than 10 (20)%. PFAAST Jacobians are poorer than those from RTIASI, although the error in the description of the central maximum is generally still less than 10% and often less than 5%. Larger errors occur in channels where there is some structure in the central maximum itself (several local maxima). Jacobians in layers where the lower sensitivity to perturbations is lower are considerably less well modelled: large relative errors are associated with poor description of the Jacobians in layers 80 to 100 (pressures less than 10 mb). This may be related to the differences in the modelled ISRF and these results should note be considered as definitive. Both models have higher type (ii) errors in the 720 and 740 cm^{-1} CO_2 Q-branch intervals.

As the altitude of the channel Jacobian maximum descends ie. at wavenumbers where maximum contributions to the outgoing longwave radiation come from lower layers in the atmosphere (see Figure 15), the maximum relative error in the description of the central maximum tends to increase: type (i) maximum errors of between 5 and 10% are observed for both models in nearly all channels with wavenumbers in the 700 to 800 cm^{-1} interval. In this interval type (ii) errors are of the order of 15% for both models. In fact this tendency persists across the window region: maximum errors of $\sim$ 10%, associated with the modelled magnitude of the central maximum, are approximately constant with wavenumber out to 920 cm^{-1}.

A similar analysis for water vapour Jacobians in the 1300 to 1450 cm^{-1} band is illustrated in Figure 18. With the exception of the 1300 to 1310 cm^{-1} interval (which poses a problem for both fast models) PFAAST gives a good description of the water vapour Jacobians: the central maximum is generally described with an error of less than 5% and overall error of less than 10%. On the other hand, RTIASI performance is poor: errors in the central maximum are of the order of 5 to 30%, and a number of channels have relative errors of the order of 1.0. The origin of these errors is illustrated in Figure 19: errors of the order of 5 to 30% are typically associated with errors in the modelled Jacobian maxima 19(a), whereas significantly larger errors are associated with discontinuities in the modelled Jacobians 19(b). These discontinuities are due to the water vapour predictor scheme 'switching' between the optically thin and optically thick regression schemes. Moreover, as illustrated in Figure 20, the occurance of the discontinuity depends (as one would expect) on the atmospheric state/water vapour content.

The PFAAST water vapour regression scheme also includes switching, but uses a different switching criteria. Jacobian discontinuities were not observed for the atmosphere and wavenumber interval tested, but that is not to say that they would not occur under different atmospheric conditions or with a different satellite viewing geometry. Switching is a generally undesirable feature of either scheme: discontinuities in the Jacobians of the type illustrated will clearly result in errors in the analysis increments and may cause problems for the minimisation routine (slow convergence, trapping in a local minimum). Water vapour predictor schemes should be developed with the continuity of the Jacobians in mind. A single regression scheme for the optically 'thin' cases and with quantifiable/predictable errors when the regression relation is used in optically thick cases may be preferable a scheme with switching and requiring further consistency tests for use within the overall assimilation process.

Before detailing further studies of the RTIASI water vapour Jacobian, one question remains outstanding: when comparing perturbations from tangent linear (RTIASI) and brute force (GENLN2) calculations (in contrast to the KCARTA/PFAAST comparisons, where both perturbations are calculated using a brute force method) the effects of nonlinearity in the RTE must be assessed. A quantitative measure of the combined effects of non-linearity and perturbations to layer average temperature mentioned above are illustrated in Figure 21. GENLN2 water vapour

[12]Bimodal Jacobians do occur in some cases, but generally there is a single mode.

Jacobians were recalculated with a perturbation d(ln$q$)=-0.01 and using CO_2 layer average temperatures. The two sets of Jacobian calculations were then compared assuming a linear scaling (by a factor of 5) of the resulting brightness temperature perturbations. The maximum differences, as defined previously, are plotted in Figure 21 and give a measure of the impact of departures from linearity. With the exception of the interval around 1305 cm^{-1}, the maximum error in the description of the central maxima is less than 5% in all cases. Type (ii) errors are also generally less than 10%. Thus we may conclude that these effects are not the major source of the discrepancies illustrated in Figure 18.

5.2 Further study of RTIASI water vapour Jacobians

In an attempt to address some of the problems with the RTIASI water vapour predictor scheme (forward model errors and Jacobian discontinuities), the November 1999 release of RTIASI included the implementation of a modified H_2O predictor scheme. In the new scheme there are three different sets of regression coefficients for water vapour and the choice of the appropriate set of coefficients depends on the transmittance of the overlying atmosphere (optically thin, optically thick and transition regimes). Comparison of water vapour Jacobians for the AFGL tropical atmosphere, as simulated by GENLN2 and the June and November 1999 releases of RTIASI are illustrated for selected channels in Figure 22. Despite very good agreement in some channels (e.g. Fig. 22a), in cases where the magnitude of the central maximum is not well described the new scheme often does not significantly improve upon the June 1999 release (graphics b and c). The November 1999 RTIASI release eliminates the Jacobian discontinuities in many cases (graphic d). In the remaining cases discontinuities are generally reduced (graphics e and f).

Water vapour Jacobian errors for the AFGL tropical atmosphere were illustrated in Figure 18. The equivalent analysis of errors in water vapour Jacobians, as calculated using the November 1999 RTIASI release on the 1300-1450 cm^{-1} interval are reproduced Figure 23. Again, large improvements are observed in channels where errors were maximum (reduction/elimination of discontinuities), but elsewhere errors in water vapour Jacobians are not changed significantly. Note that in all cases but one, type (i) errors greater than 35 % are still associated with Jacobian discontinuities. To further our understanding of the problems inherent in the water vapour Jacobians predicted by RTIASI it is necessary to consider spectroscopic and atmospheric state dependencies.

A comparison of RTIASI and GENLN2 water vapour Jacobians for the AFGL 5 sub arctic winter atmosphere are illustrated in Figure 24 for the 1300 to 1450 cm^{-1} interval. The lower continuous curve illustrates the maximum error in the description of the central maximum, as in the graphs above. The upper curves illustrate the total transmittance (continuous line) and water vapour transmittance (dotted line) from 320 hPa to space for the U. S. Standard atmosphere. This combined representation highlights two of points of interest:

- Maximum Jacobian errors for the AFGL sub arctic atmosphere are (anti)correlated with low water vapour transmittances, i.e. errors occur in the centres of moderate-to-strongly absorbed water vapour lines.
- In the 1300 to 1380 cm^{-1} interval, where type (i) and type (ii) errors are generally greater, there is strong interfering absorption (due to CH_4 and N_2O).

Considering the latter point first, it is of interest to note that the cases of discontinuity illustrated in Figures 22(d) and (f) are both associated with spectral intervals where there is interfering absorption. In the case of the 1305 cm^{-1} interval (graphic f), where CH_4 absorption is strong, the sensitivity to water vapour perturbations is very small (note the magnitude of the Jacobian elements as compared to other channels illustrated). This interval effectively does not contribute useful information on the vertical distribution of water vapour, irrespective of the Jacobian discontinuity. Thus, in this case the problem with the modelled Jacobian will not compromise IASI retrievals as such.

Case (d) in the 1340 cm^{-1} interval is more interesting: difficulties are apparantly encountered when modelling fixed gas and water vapour absorption occuring in the wings of adjacent H_2O and CH_4 lines. The November 1999 RTIASI release eliminates the discontinuity in the humid case (Figure 22f), but the description of the magnitude of the Jacobian elements is still poor. Type (i) and type (ii) errors are generally higher throughout the 1300 - 1360 cm^{-1}, and not just at the water vapour line centres. Thus, the presence of interfering absorbers may make the interpretation of absorption in the wings of water vapour lines in this spectral interval too complicated for practical (operational) use.

The occurance of maximum Jacobian[13] errors in the line centres of strongly absorbed water vapour lines are a feature of RTIASI/GENLN2 comparisons for both the dry and the humid atmospheres considered here[14]. It is also a feature of the comparison of PFAAST and KCARTA Jacobians illustrated in Figures 17 and 18. Moreover, on this spectral interval (1300 - 1450 cm^{-1}) the maximum forward model errors for both PFAAST and RTIASI

[13]Note this is true of both temperature and water vapour Jacobians.

[14]The November 1999 release AFGL tropical atmosphere water vapour Jacobians have been plotted above Figure 24 for ease of comparison.

are also associated with these water vapour lines. Future developments to the RTIASI water vapour prediction scheme cannot then realistically be expected to give improvements in these cases. Fortunately, channels centred on strong lines are not the most important for retrievals, due to their broad weighting functions. Channels in the wings of lines (within ~ 5 cm^{-1} of the line centre) are, on the contrary, of considerable interest for retrievals. In this case RTIASI water vapour Jacobian errors depend markedly on atmospheric state, as even a summary glance at Figures 23 and 24 reveals. Given that higher errors are associated with the humid profile, the representativity of the atmospheric profile set used to generate the regression coefficients for the RTIASI water vapour predictor scheme is again called into question.

Errors in water vapour Jacobians in the window region for the AFGL tropical atmosphere are illustrated in Figure 25. RTIASI's underestimation of Jacobian elements for levels at and below the Jacobian maximum is consistent with the observed cold bias in the forward model if the fast model transmittance scheme predicts an optically thicker atmosphere (H_2O) than GENLN2. This hypothesis has been verified by direct comparison of GENLN2 and RTIASI water vapour transmittance calculations. The smooth variations of the forward model and Jacobian errors with wavenumber are strongly suggestive of a problem in the representation of the water vapour continuum. It would be of real interest to know wether these errors could be improved by separating out the water vapour continuum contribution in the water vapour transmittance predictor scheme. Unfortunately equivalent calculations have not been performed for PFAAST to date.

To conclude with regard to the accuracy of the RTIASI analytic Jacobians, with the exception of the window region and in the centres of strongly absorbed water vapour lines, temperature Jacobians are well reproduced. Water vapour Jacobians in the centres of strong lines are not well described, and discontinuities still arise with the November 1999 release. However, it is argued that these channels could be excluded from assimilation without significant loss of information because the weighting functions for channels centred on strong absorption lines will generally be very broad. Moreover, forward model errors are greatest for these channels. The marked degradation of the accuracy of water vapour Jacobians in line wings in the tropical atmosphere is a however a serious source of concern. Errors in this case are typically of the order of 10 to 20 % and will clearly compromise the accuracy of retrievals. Shortcomings in the modelled water vapour absorption (specifically the dry bias in the profile set used to generate the RTIASI water vapour predictors) are called into question, and are also believed to be the origin of poorly modelled temperature and water vapour Jacobians in the window region. It is hoped that the anticipated rederivation of the water vapour regression coefficients using a revised profile set will significantly improve the accuracy of the water vapour transmittance scheme. Separate prediction of the water vapour continuum absorption may also be advantageous.

The accuracy of the PFAAST brute force Jacobians is generally satisfactory (c.f. comments on strong water vapour lines above). Performance in the 600 to 800 cm^{-1} interval would require further attention, were this model to be adopted for NWP purposes, once discrepancies in the definition of the ISRF are resolved. The lack of any analytic means to calculate Jacobian elements is however a significant shortcoming of the PFAAST model, given UKMO requirements for variational assimilation.

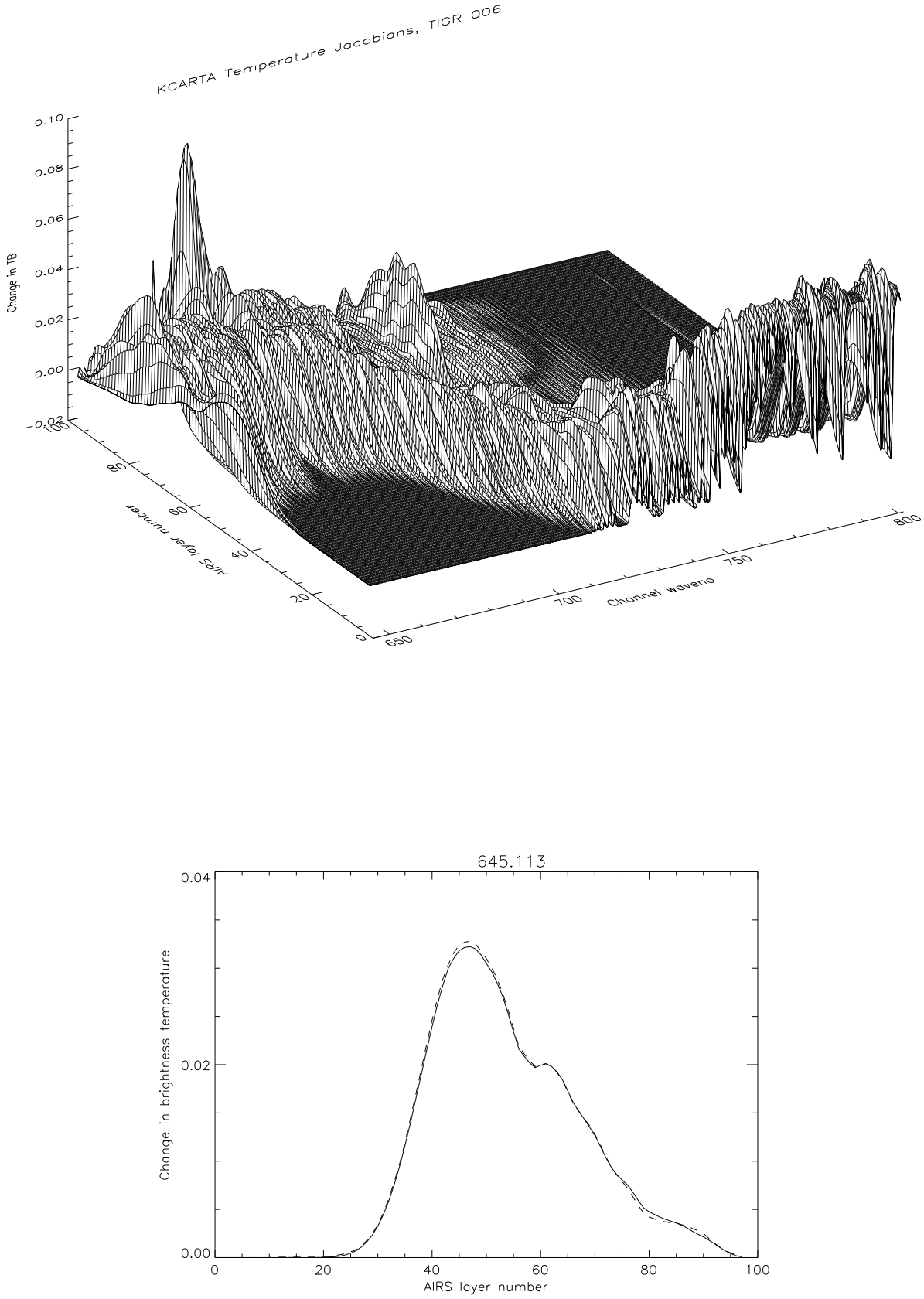

Figure 15: Temperature Jacobians calculated using KCARTA for TIGR profile 006 in the 645 to 800 cm^{-1} wavenumber interval. In the lower graph a cross section through the surface at 645.113 cm^{-1} (solid line) and the equivalent PFAAST brute force Jacobian for this channel (dashed line) are illustrated.

Temperature Jacobians 645 to 800 cm^{-1}

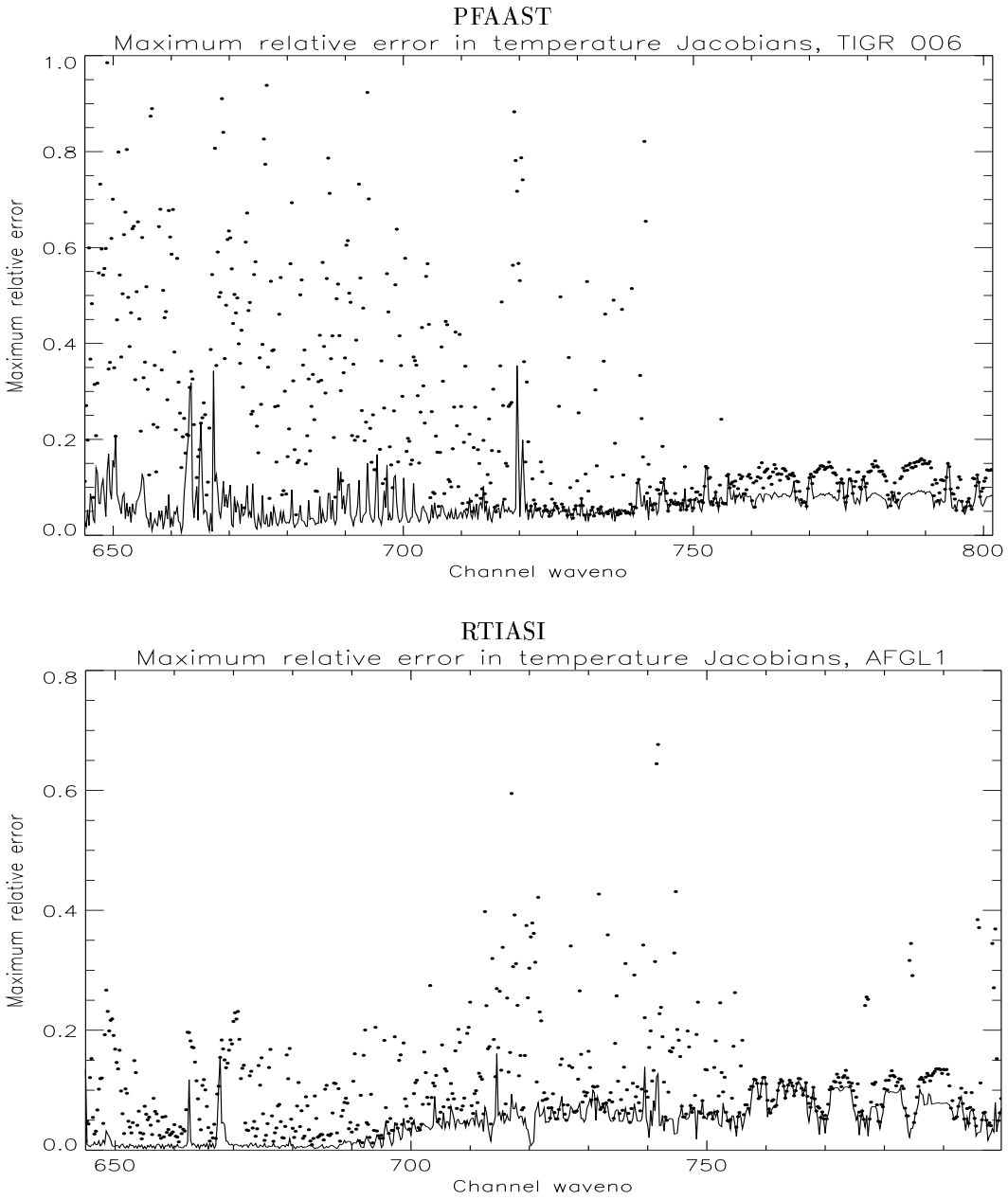

Figure 16: Maximum relative error in the temperature Jacobians on the 645 to 800 cm^{-1} interval. Each fast model is compared to its own generator. The calculations illustrated are for a tropical atmosphere. The maximum relative error (i) for levels where the change in brightness temperature is $\geq$ 0.5 MaxΔTB and (ii) for levels where the change in brightness temperature is $\geq$0.1 MaxΔTB are traced with lines and dots respectively.

Temperature Jacobians 1300 to 1450 cm^{-1}

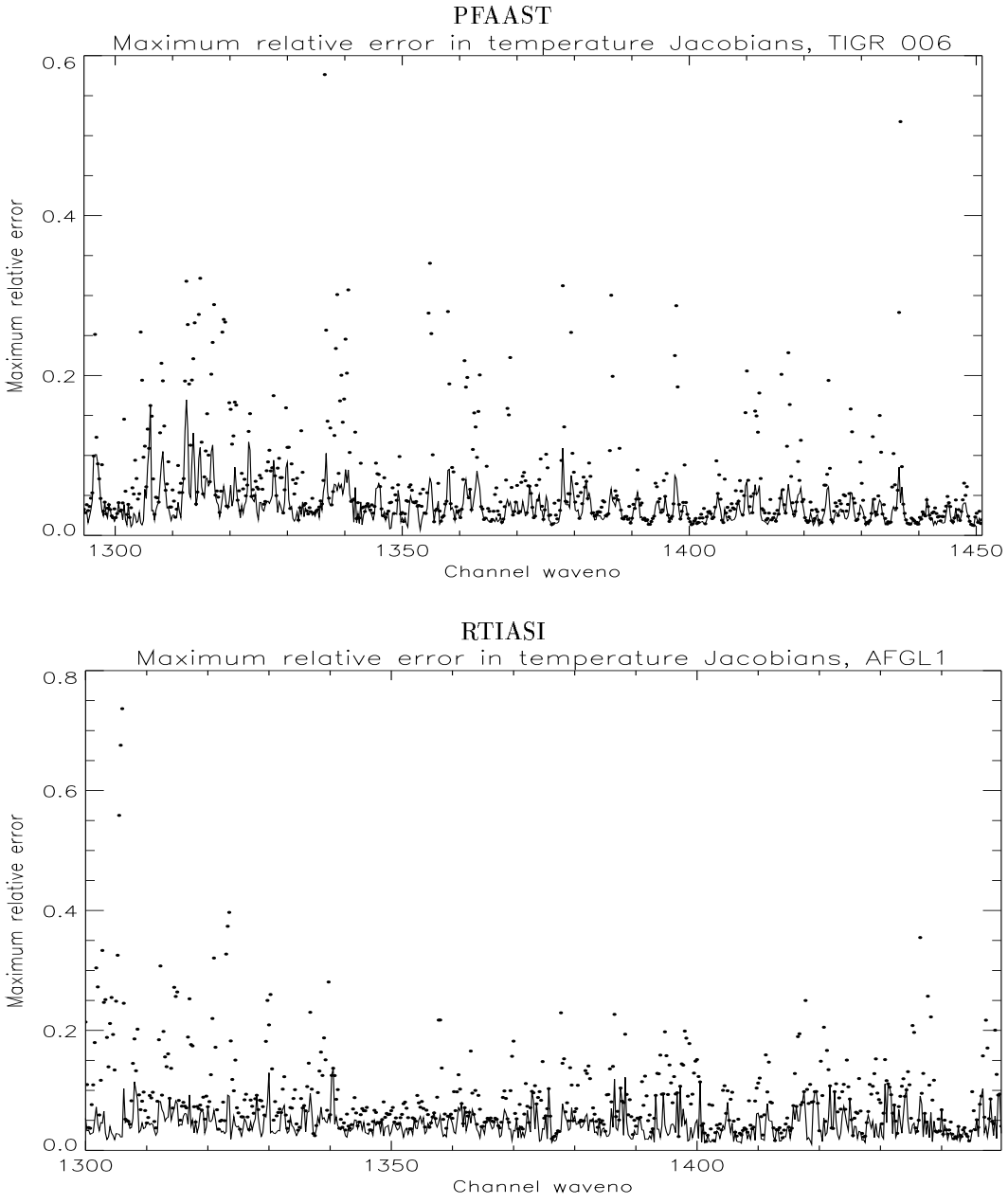

Figure 17: Maximum relative error in the temperature Jacobians on the 1300 to 1450 cm^{-1} interval. All details and symbols as in Figure 16.

H_2O Jacobians 1300 to 1450 cm^{-1}

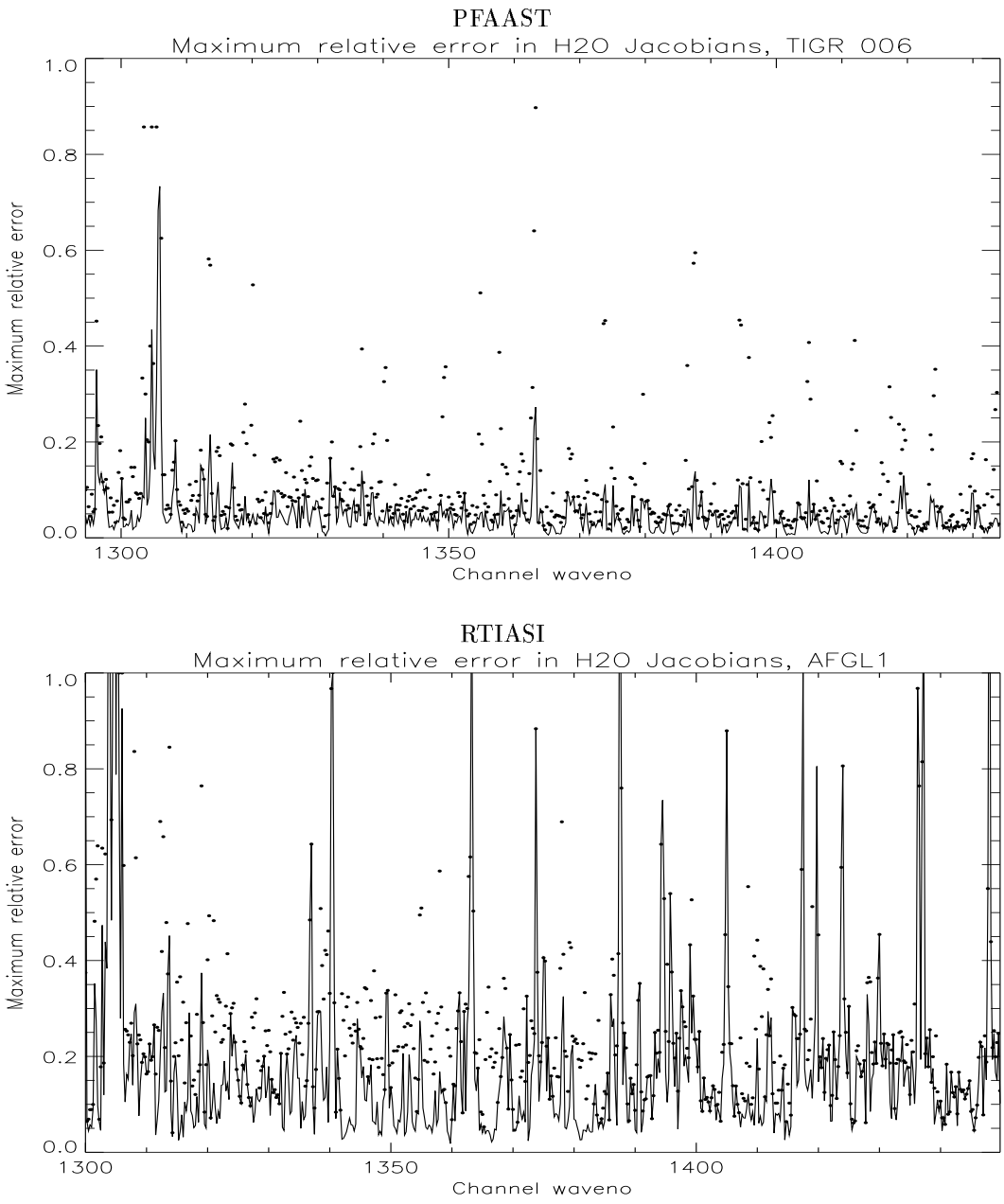

Figure 18: Maximum relative error in the water vapour Jacobians on the 1300 to 1450 cm^{-1} interval. All details and symbols as in Figure 16.

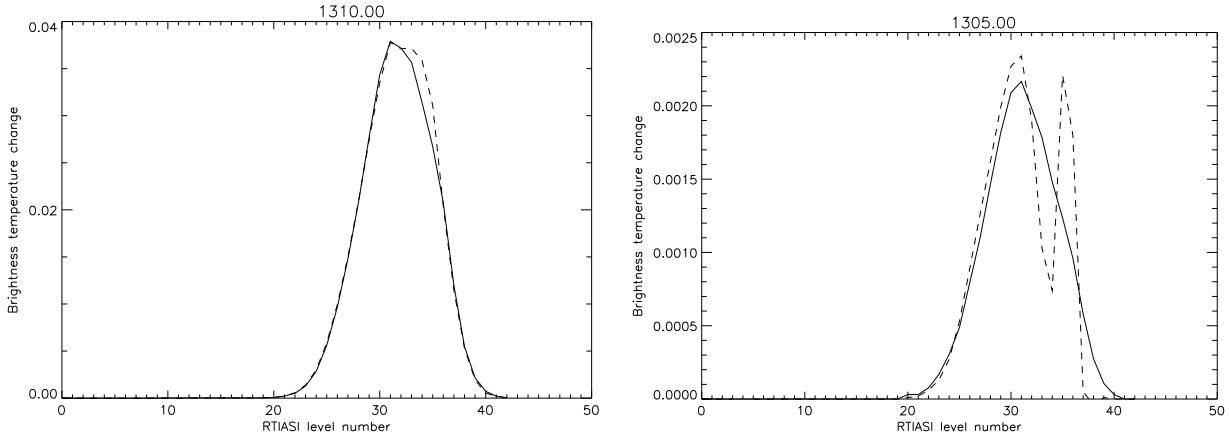

Figure 19: RTIASI Jacobians for channels at (a) 1310 and (b) 1305 cm^{-1} illustrating errors in the modelling of the magnitude and form of the local maximum, and errors associated with discontinuities in the fast model Jacobians (dashed curve). GENLN2 Jacobians are illustrated with a solid line.

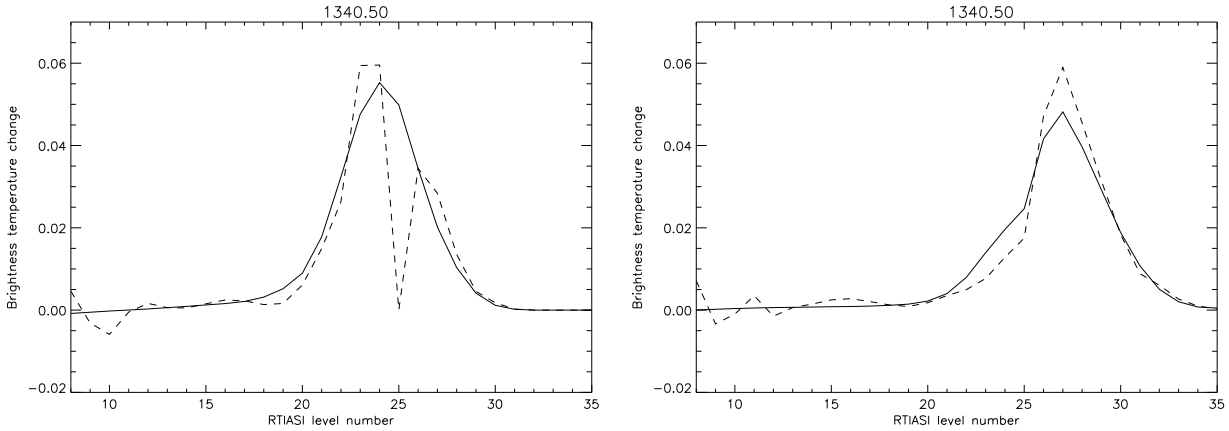

(a) AFGL Tropical Atmosphere (b) AFGL Sub Artic Winter Atmosphere

Figure 20: RTIASI Jacobians for the channel at 1340.5 cm^{-1} for (a) the AFGL tropical atmosphere and (b) the AFGL sub arctic winter atmosphere. The occurance of Jacobian discontinuities depends on atmospheric conditions - in particular the water vapour content.

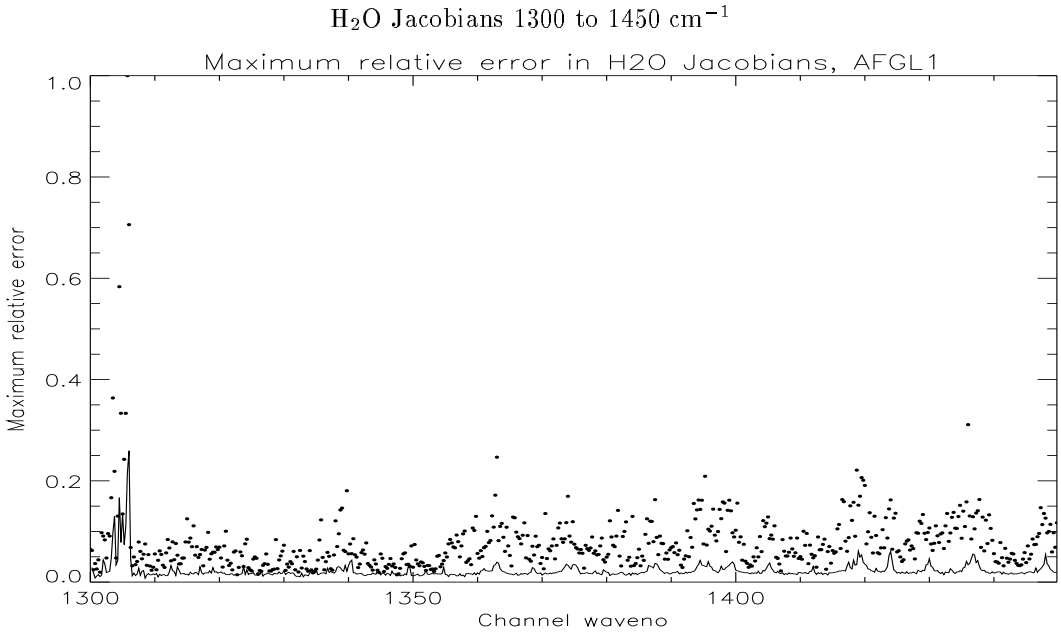

Figure 21: Quantification of the effects non-linearity and layer average temperature modifications on the maximum relative error in the water vapour Jacobians on the 1300 to 1450 cm^{-1} interval for the AFGL Tropical atmosphere. GENLN2 brightness temperature perturbations have been calculated from simulations (i) with d(ln$q$)=-0.05 and Curtis Godson layer average temperatures and (ii) with d(ln$q$)=-0.01 and CO_2 layer average temperatures. These calculations are then compared assuming a linear scaling of the brightness temperture perturbation. The maximum errors defined previously give a measure of the error inherent in this assumption and are illustrated here. The effects of non-linearity are much less than other sources of error for RTIASI.

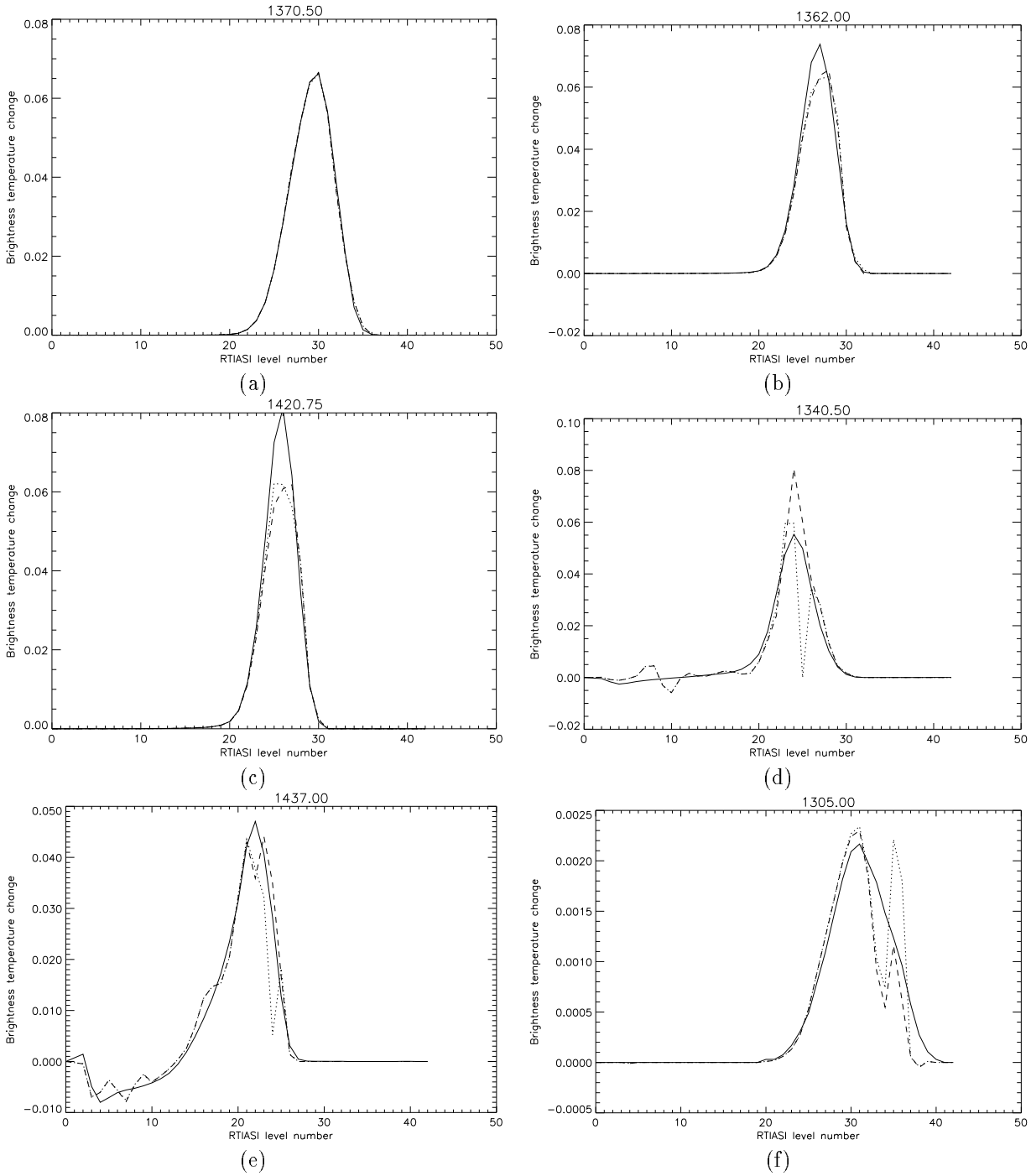

Figure 22: Water vapour Jacobians for selected IASI channels simulated for the AFGL Tropical atmosphere using the June and November 1999 releases of RTIASI (dotted and dashed lines respectively). Genln2 Jacobians are illustrated with continuous lines as previously. The three-case water vapour regression scheme improves Jacobian discontinuities in most, but not all cases. Large errors in the magnitude of the central maximum still remain, as illustrated in graphics (b) and (c).

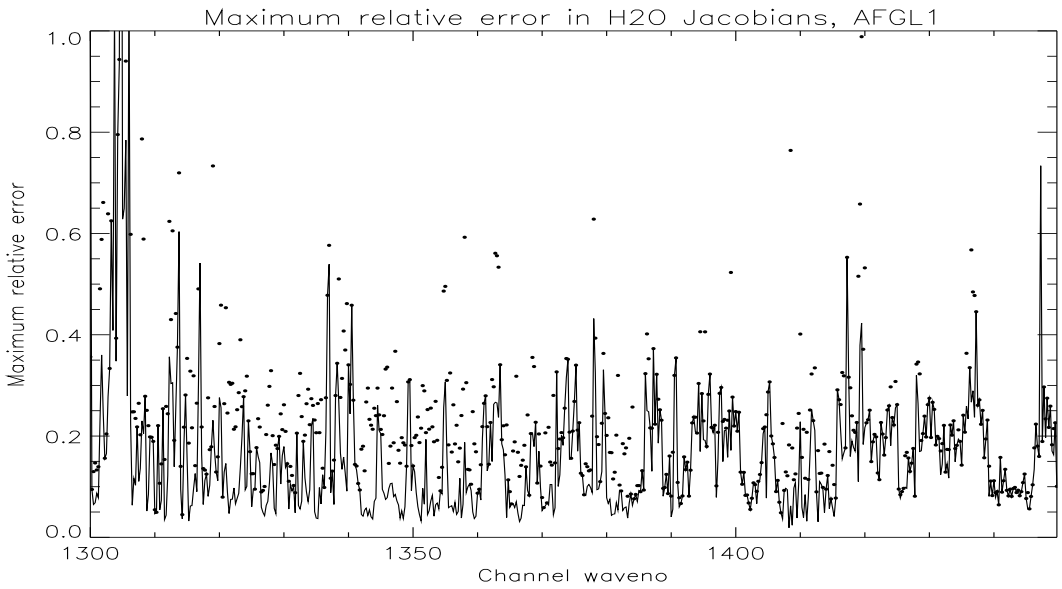

Figure 23: Maximum relative error in the water vapour Jacobians on the 1300 to 1450 cm^{-1} interval for the AFGL Tropical atmosphere calculated with the November 1999 release of RTIASI. All details and symbols as in Figure 16.

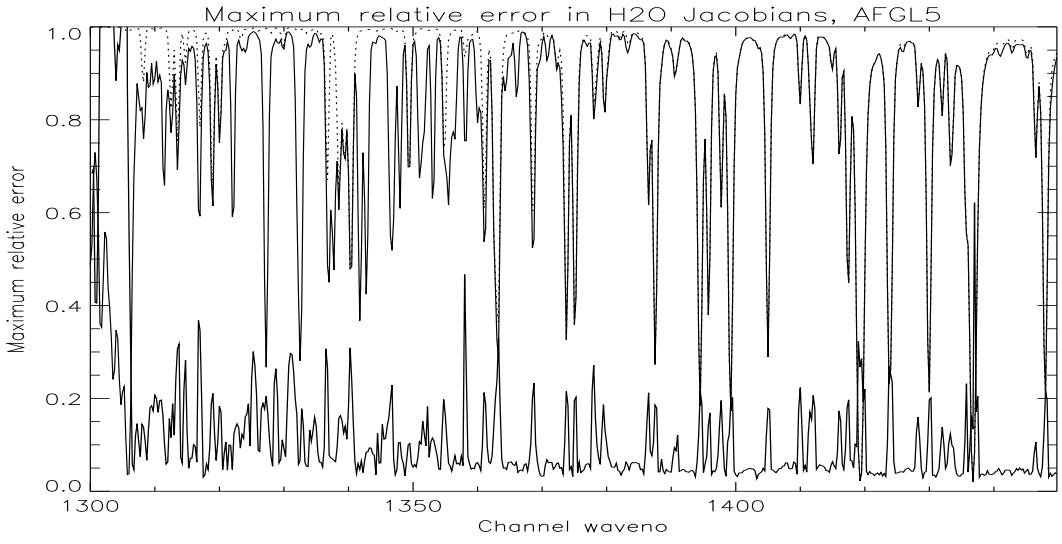

Figure 24: Maximum relative error in the water vapour Jacobians on the 1300 to 1450 cm^{-1} interval for the AFGL sub-arctic winter atmosphere. The lower solid line represents the maximum error in the description of the Jacobian central maxima, as previously. The upper solid and dotted curves illustrate total transmittances and water vapour transmittances from 320 mb to space respectively. These transmittances were simulated using the June 1999 release of RTIASI for the U. S. Standard atmosphere and are only intented to give an indication of spectral intervals where there is moderate to strong water vapour absorption.

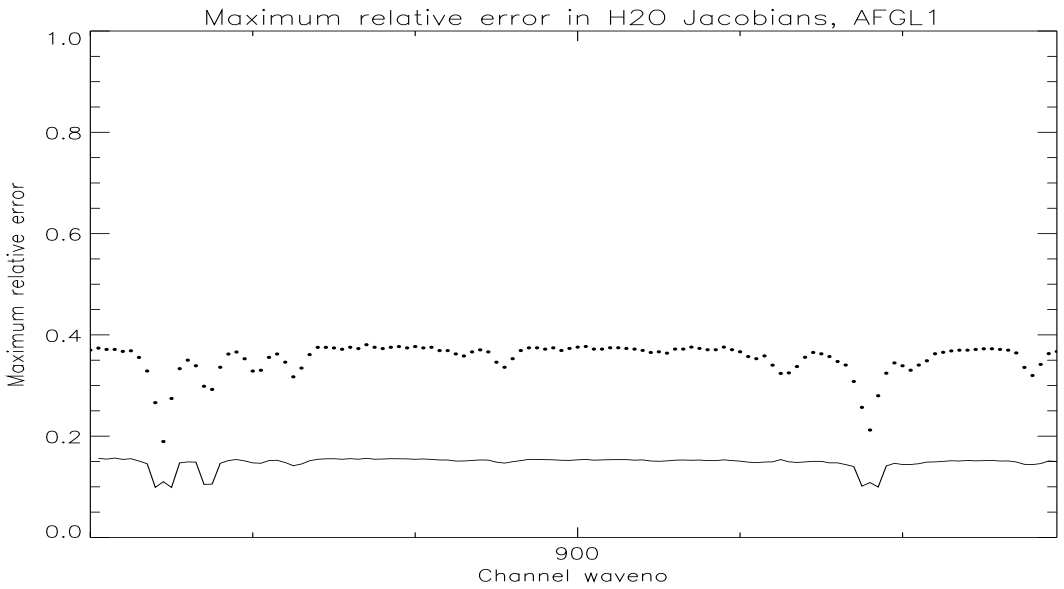

Figure 25: Maximum relative error in the water vapour Jacobians on the 885 to 915 cm^{-1} interval for the AFGL Tropical atmosphere. All details and symbols as in Figure 16.

6 Conclusions

Forward model errors and Jacobians have been compared for two existing pressure level optical depth IASI fast models, RTIASI and PFAAST, for a small representative set of atmospheric profiles. Overall the forward model error characteristics are satisfactory. On spectral intervals of interest for atmospheric sounding most channels have forward model errors which are significantly lower than instrumental noise, ie. forward modelling uncertainties do not compromise the information content of the satellite observations. Temperature Jacobians are also generally well described by both models. However, the models tested each have specific problems and/or limitations and revision of both models will probably be required before they are adequate for integration in an operational data assimilation system.

The RTIASI model has good forward model error characteristics in the 15 and 4.3 μm CO_2 bands (temperature sounding). Temperature Jacobians are well modelled in the 15μm CO_2 and 6.7μm H_2O bands (Jacobians were not calculated for the 4.3μm band). Forward model error characteristics are slightly poorer and temperature Jacobians slightly less well represented in the window region. The degradation in performance would appear to be linked to the modelling of water vapour absorption in the lower troposphere. RTIASI forward model errors in the H_2O ν_2 band are greater than those for PFAAST due to the combined effects of vertical resolution and transmittance errors. The study presented here suggests that the mode of water vapour absorption in RTIASI leads to forward model errors which are spectrally correlated and whose magnitude depends on atmospheric state; performance is worst in humid atmospheres. Errors in predicted water vapour transmittances can also give rise to large errors (and even discontinuities) in modelled Jacobians in the centre and near wing of water vapour lines. Again, the magnitude of errors and their degree of spectral correlation depends on atmospheric state. The representativity of the profile set used to generate the regression coefficients for the water vapour predictor scheme is called into question. A revision of the RTIASI water vapour predictor scheme appears necessary.

The accuracy of PFAAST Level 1C radiance calculations is compromised by the instrumental spectral response function and spectral resolution used to generate the fast model transmittance predictor scheme. When PFAAST is assessed against high resolution spectra which are convolved with the PFAAST ISRF then forward model errors and modelled Jacobians are comparable or better than those from RTIASI, with the exception of the 12 to 15 μm interval. Given the performance of the PFAAST PLOD model in the H2O ν_2 band and the instrument noise levels there is probably no real need to use the OPTRAN method for IASI - the PFAAST results would indicate that with adequate vertical resolution and/or accurate transmittance predictors the water vapour absorption is well modelled in all but the strongest lines. Given the requirements (of a fast model) for variational data assimilation, the lack of a means to generate analytic Jacobians is a serious shortcoming of the PFAAST model.

Thus, despite the potential shortcomings of the RTIASI model, this is the model which is currently selected for the development of a 1D-VAR retrieval scheme. In the short term work should focus on:

- specification of the forward model error covariance matrix F,
- assesment of the impact of correlated forward model error on retrievals,
- and assessment of the impact of the errors in the H_2O Jacobians on retrievals.

Recommendations for revision of the fast radiative tranfer model, if required, should be based on the outcome of these studies. Specifically, the estimation of the forward model error covariance matrix will require:

- rerunning high vertical resolution GENLN2 simulations with interpolation issues eliminated/solved,
- treatment of the climatological variation of N_2O (CH_4, CO) and the effect of missing gases (HNO_3 for example),
- extension of radiance simulations to a larger sample of atmospheric states, particularly for the estimation of correlations and assessment of state dependent forward model errors,
- estimation/treatment of characteristic spectroscopic errors.

All but the latter task are straight-forward, but they are (computer) time intensive to a lesser (1,2) or greater degree (3,4).

References

[1] F. Cayla. Simulation of IASI spectra. Technical Report IATN-0000-5627-CNE, Centre Nationale d'Etudes Spatiales, Toulouse, France, 1996.

[2] M. Matricardi and R. Saunders. Fast radiative transfer model for simulation of infrared atmospheric sounding interferometer radiances. *Appl. Optics*, 38(27):5679–5691, 1999.

[3] F. Aires, R. Armante, A. Chedin, and N. A. Scott. Surface and atmospheric temperature retrieval with the high resolution interferometer IASI. In *9th Conference on Satellite Meteorology and Oceanography*, pages 181–186, 1998.

[4] S. Hannon, L. Larrabee Strow, and W. W. McMillan. Atmospheric infrared fast transmittance models: a comparison of two approaches. In *Optical Spectroscopic Techniques and Instrumentation for Atmospheric and Space Research*, pages 94–105, 1996.

[5] Technical Report IATN-0000-5479-CNE, Centre Nationale d'Etudes Spatiales, Toulouse, France, 1996.

[6] C. D. Barnet and J. Susskind. Simulation studies of advanced infrared and microwave sounders. In *ITSC-10*, 1999.

[7] M. T. Chanine, H. Aumann, M. Goldberg, E. Kalnay, L. McMillan, P. Rosenkranz, D. Staelin, L. Larrabee Strow, and J. Susskind. Algorithm theoretical basis document, AIRS-team unified retrieval for core products. Technical report, 1997.

[8] A. Amato *et al.* Inverting for geophysical parameters from img radiances. *IEEE transactions on geoscience and remote sensing*, 37(3):1625–, 1999.

[9] Y. Han, J. A. Shaw, J. H. Churnside, P. D. Brown, and S. A. Clough. Infrared spectral radiance measurements in the tropical pacific atmosphere. *J. Geo. Res.*, 102(D4):4353–4356, 1997.

[10] A. Chedin, N. A. Scott, C. Wahiche, and P. Moulnier. The improved initialisation inversion method: a high resolution method for temperature retrievals from satellites of the TIROS-N series. *J. Clim. Appl. Meteorol.*, 24:128–143, 1985.

[11] S. de Souza-Machado, L. Larrabee Strow, H. Motteler, and S. Hannon. kCARTA: an atmospheric radiative transfer code using compressed lookup tables. Technical report, Physics Department, Uiniversity of Maryland Baltimore County, Baltimore MD21250, USA, 1998.

[12] D. C. Tobin, L. Larrabee Strow, W. J. Lafferty, and W. B. Olson. Experimental investigation of the self and n_2 broadened continuum within the ν_2 band of water vapour. *Appl. Optics*, 35(24):4724–4734, 1996.

[13] R. W. Saunders. How good is the tangent linear approximation for satellite observation operators. In *ECMWF Workshop on Data Assimilation*.